



Research paper

Synthesis and biological evaluation of novel chalcone derivatives as a new class of microtubule destabilizing agents



Xiaochao Huang^{a, b, 1}, Rizhen Huang^{a, b, 1}, Lingxue Li^{a, b}, Shaohua Gou^{a, b, *}, Hengshan Wang^{c, **}

^a Pharmaceutical Research Center and School of Chemistry and Chemical Engineering, Southeast University, Nanjing 211189, China

^b Jiangsu Province Hi-Tech Key Laboratory for Biomedical Research, Southeast University, Nanjing 211189, China

^c State Key Laboratory for the Chemistry and Molecular Engineering of Medicinal Resources (Ministry of Education of China), School of Chemistry and Pharmaceutical Sciences of Guangxi Normal University, Guilin 541004, China

ARTICLE INFO

Article history:

Received 13 November 2016

Received in revised form

14 February 2017

Accepted 15 March 2017

Available online 18 March 2017

Keywords:

Chalcone

Tubulin

Molecular modeling

Anti-tumor activity

Apoptosis

ABSTRACT

A series of novel chalcone derivatives were designed and synthesized as potential antitumor agents. Structures of target molecules were confirmed by ¹H NMR, ¹³C NMR and HR-MS, and evaluated for their *in vitro* anti-proliferative activities using MTT assay. Among them, compound **12k** displayed potent activity against the test tumor cell lines including multidrug resistant human cancer lines, with the IC₅₀ values ranged from 3.75 to 8.42 μM. In addition, compound **12k** was found to induce apoptosis in NCI-H460 cells via the mitochondrial pathway, including an increase of the ROS level, loss of mitochondrial membrane potential, release of cytochrome c, down-regulation of Bcl-2, up-regulation of Bax, activation of caspase-9 and caspase-3, respectively. Moreover, the cell cycle analysis indicated that **12k** effectively caused cell cycle arrest at G2/M phase. The results of tubulin polymerization assay displayed that **12k** could inhibit tubulin polymerization *in vitro*. Furthermore, molecular docking study indicated that **12k** can be binding to the colchicine site of tubulin.

© 2017 Published by Elsevier Masson SAS.

1. Introduction

Microtubules, as key components of the cytoskeleton, are cytoskeletal filaments consisting of α , β -tubulin heterodimers and involved in a series of cellular processes including regulation of motility, cell signaling, maintenance of cell shape, cell proliferation and intracellular transport [1–4]. Since microtubules play an important role in the life cycle of the cell, they have been considered as a major target for the development of novel anticancer agents in recent years [5–7]. In recent decades, numbers of compounds as anti-mitotic agents derived from natural sources or obtained by chemical synthesis have been reported [8–10]. In general, these compounds were divided into three major types such as the taxane site for microtubule stabilizing agents, the vinca site, and the colchicine site for microtubule polymerization inhibitors

[11–13]. Anti-mitotic agents including taxanes and vinca alkaloids have been widely used for the treatment of a variety of cancers in the past decade [14,15]. However, the clinical use of these compounds was always limited by the high toxicity, the development of drug resistance, side effects, poor solubility, low oral bioavailability and complex synthesis [15,16]. Therefore, scientists are eager to develop and discover novel effective anti-mitotic agents for overcoming the above mentioned drawbacks.

Natural products and their derivatives provide a diverse source of new medicinal leads and they play a major role in drug development, especially in the area of cancer therapy [17]. Chalcones are naturally occurring moieties of flavonoid and isoflavonoid compounds, which are an important pharmacophore of many natural products including curcumin, flavokawain, millepachine, and xanthohumol [18–21]. In addition, many researchers reported that chalcone and its analogues also exhibited wide range of biological activities, such as anti-oxidant, anti-filarial, anti-bacterial, anti-fungal, anti-mitotic, anti-tumor, anti-inflammatory and inhibition of enzymes activities [22–29]. Millepachine, as a novel chalcone with a 2,2-dimethylbenzopyran motif (**1a**, Fig. 1) which was first isolated from the *Milletia pachycarpa* by Chen and co-workers in

* Corresponding author. Jiangsu Province Hi-Tech Key Laboratory for Biomedical Research, Southeast University, Nanjing 211189, China.

** Corresponding author.

E-mail addresses: sgou@seu.edu.cn (S. Gou), whengshan@163.com (H. Wang).

¹ Co-first author: These authors contributed equally to this work.

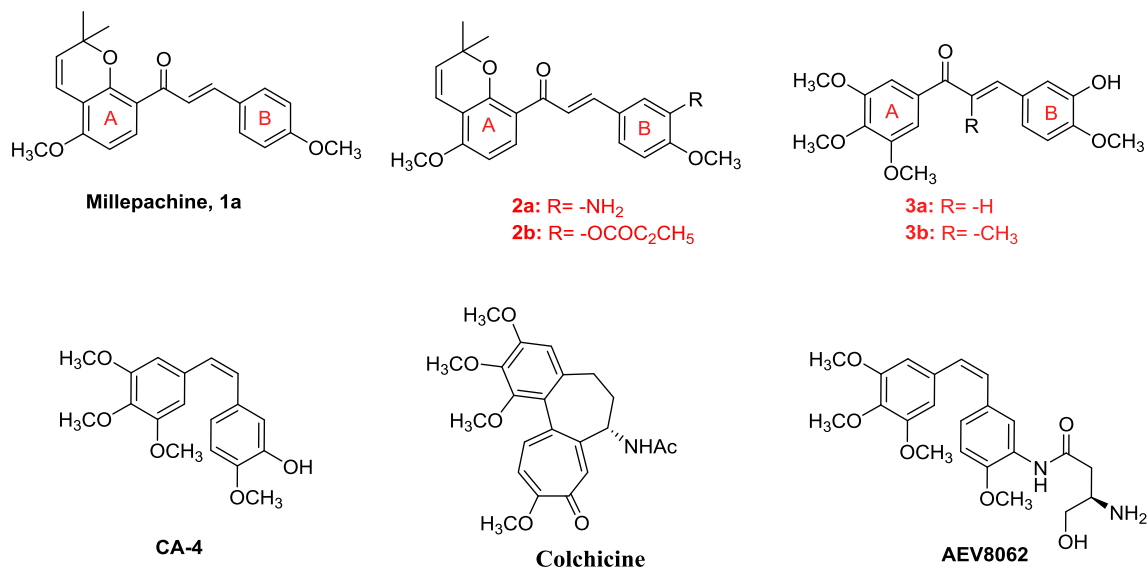


Fig. 1. Structures of natural products and chalcone analogues as potent inhibitors of tubulin polymerization.

2013, has been known to exert potent cytotoxicity *in vitro* against a variety of cancer cells and potent *in vivo* antitumor activity [30]. In order to improve the antitumor activity of millepachine, during the last a few years, Chen and co-workers have explored the B-ring of millepachine with different substituted groups, such as introduction of hydroxyl group on the B-ring of millepachine or replacement of methoxyl with diethyl amine, to result in improvement on their antitumor activity [21,31]. In previous work, a number of millepachine derivatives were designed and synthesized as potential anticancer agents [15,21,30–33]. Among them, compound **2a** (Fig. 1) and **2b** displayed excellent antitumor activities toward various human cancer cell lines including multidrug resistant ones *in vitro* and *in vivo*, and strongly inhibited tubulin polymerization by binding to the colchicine site of tubulin. However, pharmacokinetic studies indicated that low oral bioavailability of these compounds has limited further study. In addition, compounds **3a** and **3b** (Fig. 1), as a combretastatin A-4 analogous chalcone, were reported to have potent antitumor activities against a panel of cancer cell lines and markedly inhibit the polymerization of tubulin [34,35]. These encouraging results prompted us to further design and synthesize a new class of chalcone derivatives as potential anticancer agents.

In an effort to discover more effective compounds that target the tubulin-microtubule system as a tubulin de-polymerization inhibitor, we have designed and synthesized a new series of chalcone derivatives and evaluated their antitumor activities in the present study. Among all the compounds, compound **12k** displayed the most potent antitumor activity against the tested cancer cell lines including multidrug resistant phenotype, and effectively induced cell cycle arrest in G₂/M phase. Moreover, molecular docking analysis was made to examine whether compound **12k** could inhibit the polymerization of tubulin by binding to the colchicine binding site.

2. Results and discussion

2.1. Chemistry

The general procedures for the synthesis of chalcone derivatives are described in Schemes 1 and 2. Compounds **1–4** and **9** were synthesized according to the reported procedures [15,21,35].

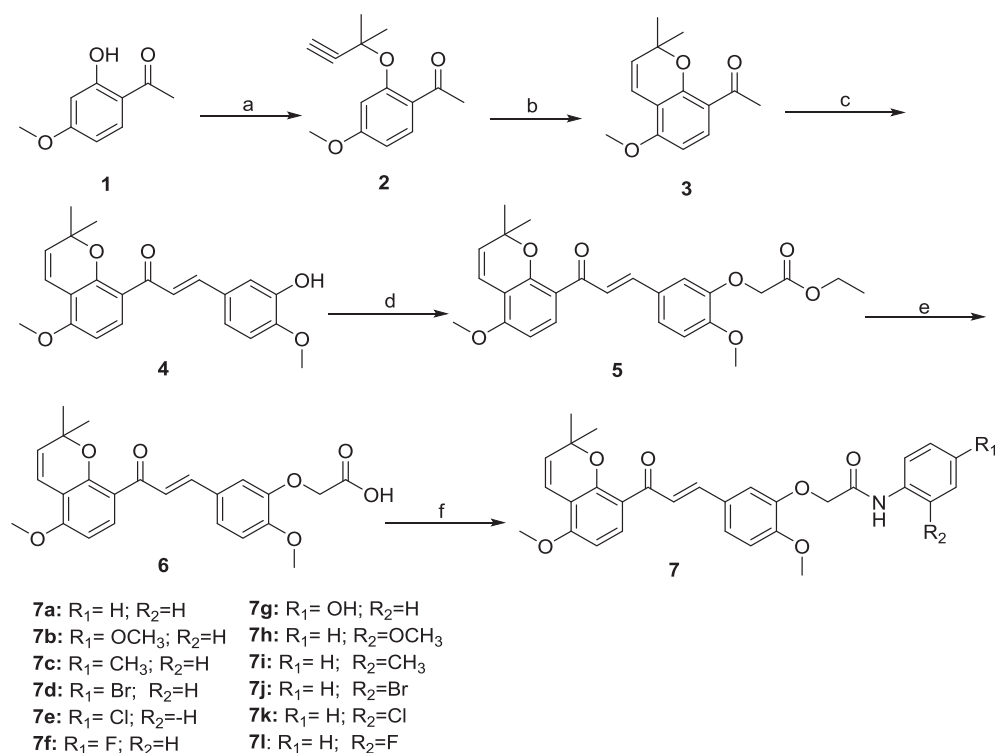
Treatment of compound **1** with 3-chloro-3-methyl-1-butene in the presence of DBU and catalytic amounts of CuCl₂·2H₂O in CH₃CN afforded the intermediate **2** (yield, 76.1%). The resulting compound **2** was cyclized by heating in pyridine to produce the key intermediate **3** (yield, 73.3%). Subsequently, Claisen-Schmidt condensation of **3** or **8** with 3-hydroxy-4-methoxybenzaldehyde in the presence of KOH in CH₃OH led to the production of the intermediate **4** (yield: 65.2%) or **9** (yield, 54.8%), which was upon etherification with α -bromoethyl acetate, K₂CO₃ and KI in the presence of DMF to give ester **5** (yield, 93.3%) or **10** (yield, 90.9%) followed by its hydrolysis with aluminum hydroxide in the presence of THF/H₂O to generate the acid **6** (yield, 95.0%) or **11** (yield, 91.9%). Finally, target compounds **7a–7l** (yields, 52.3%–95.2%) and **12a–12l** (yields, 43.1%–95.6%) were achieved by the formation of amide bond between **6** or **11** and anilines, respectively, in the presence of HOBT/EDCI. The structures of these target compounds were confirmed by ¹H NMR, ¹³C NMR and high resolution mass spectra (HR-MS).

2.2. Biology activity

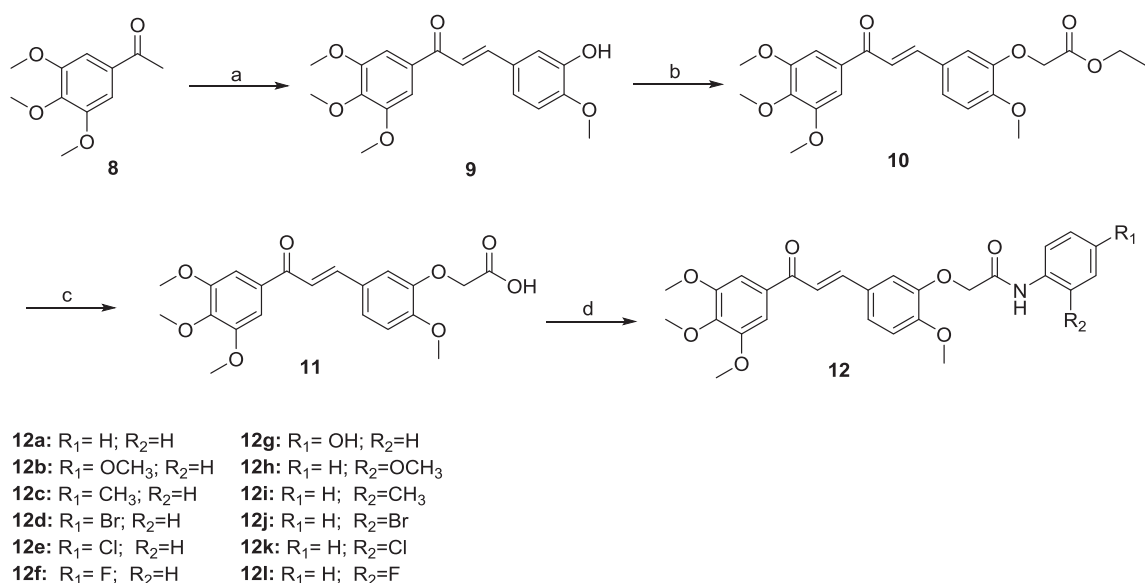
2.2.1. Cytotoxicity test

The *in vitro* inhibitory effect of these synthesized chalcone derivatives was evaluated by MTT assay against HepG-2, NCI-H460, MGC-803, SK-OV-3 and T-24 cancer cell lines together with HL-7702 normal cell line, and compound **1a** (Millepachine) was chosen as reference. The IC₅₀ values obtained in the performed *in vitro* inhibition assays are summarized in Table 1.

As shown in Table 1, the newly synthesized chalcone derivatives are potent anticancer agents, with IC₅₀ values mostly in the micromole level. Among all compounds, it was notable that compound **12k** exhibited the best antitumor activity against HepG-2, NCI-H460, SK-OV-3 and T-24 cancer cells and had low cytotoxicity on normal human cell line (HL-7702) compared with compound **1a**. The results revealed that the analogues **7b** and **7c**, obtained by inserting a methoxy or methyl moiety in the position 4 of the lateral benzene group, led to significant increase in potency compared with other analogues substituted by halogen. Compound **7b**, with IC₅₀ value of 6.73 μ M against MGC-803 cells, was about 3-fold more active than derivatives **7d** and **7e**, and undoubtedly emerged as one of the most active compounds within this subset. **7c** containing a methyl group in the 4-position had an IC₅₀ of 8.23 μ M in the same



Scheme 1. Synthetic pathway to prepare target compounds **7a-7l**: Reagents and conditions: (a) 3-Chloro-3-methylbut-1-yne, CuCl₂·2H₂O, DBU, CH₃CN, 0 °C, 12 h. (b) Pyridine, 120 °C, 12 h (c) KOH (50% w/v aqueous solution), 3-hydroxy-4-methoxybenzaldehyde, CH₃OH, 0 °C, 12 h (d) α -bromoethyl acetate, K₂CO₃, KI, DMF, rt, overnight. (e) LiOH·H₂O, THF/H₂O, rt, 2 h (f) HOBT, EDCI, DMF, rt, overnight.



Scheme 2. Synthetic pathway to prepare target compounds **12a-12k**: Reagents and conditions: (a) KOH (50% w/v aqueous solution), 3-hydroxy-4-methoxybenzaldehyde, CH₃OH, 0 °C, 12 h (b) α -bromoethyl acetate, K₂CO₃, KI, DMF, rt, overnight. (c) LiOH·H₂O, THF/H₂O, rt, 2 h (d) HOBT, EDCI, DMF, rt, overnight.

cell line. A beneficial effect was also observed with the modifications of the C-2 position. The derivative **7h** was 4-fold more active than **7j** against NCI-H460. The presence of a weakly electron-withdrawing and bulky group in position C-2 and C-4 seemed to be associated with a general increase in activity within **7** series. Furthermore, in the second series of compounds, **12b** owning a methoxy substituent in the para-position of the lateral benzene ring also had significant activity against the selected cancer cell

lines, with an IC₅₀ range from 7.07 to 9.82 μ M. It was important to note that compounds **12j-12l**, possessing a halogen substituent in the C-2 position of the benzene ring, showed reverse effects as compared with **7j-7l**, indicating that the electron-withdrawing group might be suitable for this position. Moreover, the modifications of 4-position of the lateral phenyl ring with a halogen or hydroxy moiety caused loss of potency, for example, compound **12b** exhibited better cytotoxicity activities than **12d-12g** against the test

Table 1
Effects of chalcones derivatives **7** and **12** against different cell lines.

Compd.	IC ₅₀ (μM) ^a					
	HepG-2	NCI-H460	MGC-803	SK-OV-3	T24	HL-7702
7a	20.62 ± 1.22	17.57 ± 0.94	18.36 ± 1.08	20.78 ± 1.23	21.09 ± 0.86	>50
7b	8.99 ± 1.20	8.56 ± 0.99	6.73 ± 1.14	9.02 ± 0.96	9.51 ± 0.92	>50
7c	9.32 ± 1.16	8.77 ± 1.04	8.23 ± 1.00	9.58 ± 1.11	10.13 ± 1.38	>50
7d	22.74 ± 1.08	20.46 ± 0.88	17.22 ± 0.98	18.96 ± 1.07	19.87 ± 1.24	>50
7e	15.38 ± 1.15	12.88 ± 1.10	19.35 ± 1.07	20.01 ± 1.12	17.12 ± 1.22	>50
7f	14.09 ± 0.89	14.24 ± 1.12	13.49 ± 0.48	13.86 ± 0.86	17.64 ± 1.01	>50
7g	15.62 ± 1.27	17.98 ± 0.97	20.85 ± 1.04	14.47 ± 1.09	18.34 ± 0.98	>50
7h	7.35 ± 0.79	5.48 ± 1.14	6.72 ± 0.95	8.24 ± 0.86	7.84 ± 1.21	>50
7i	9.44 ± 0.78	7.96 ± 0.77	10.34 ± 0.83	10.02 ± 0.84	9.86 ± 0.96	>50
7j	27.80 ± 1.02	20.04 ± 1.09	32.72 ± 1.23	30.28 ± 1.21	23.25 ± 1.15	>50
7k	11.82 ± 1.17	12.95 ± 1.01	14.18 ± 1.19	14.56 ± 1.08	15.43 ± 0.43	>50
7l	19.12 ± 1.25	16.97 ± 1.13	20.56 ± 1.06	18.71 ± 1.24	17.49 ± 0.91	>50
12a	10.14 ± 1.32	11.28 ± 0.94	14.55 ± 0.75	10.67 ± 1.36	12.58 ± 0.51	>50
12b	7.66 ± 0.71	7.07 ± 0.81	8.52 ± 0.89	9.82 ± 0.93	9.36 ± 0.72	>50
12c	8.97 ± 0.97	7.69 ± 1.07	10.34 ± 1.32	10.28 ± 1.29	11.56 ± 0.94	>50
12d	10.46 ± 1.05	10.27 ± 0.64	12.90 ± 1.43	13.05 ± 1.33	11.61 ± 1.31	>50
12e	20.53 ± 1.52	20.12 ± 1.55	26.30 ± 1.38	27.15 ± 1.49	21.73 ± 1.26	>50
12f	21.23 ± 1.29	19.18 ± 1.36	20.92 ± 1.20	22.47 ± 1.35	24.65 ± 0.66	>50
12g	>50	>50	36.63 ± 1.13	>50	>50	>50
12h	13.57 ± 1.30	12.09 ± 1.27	14.93 ± 1.18	16.18 ± 0.65	17.45 ± 1.52	>50
12i	26.27 ± 1.21	22.86 ± 0.98	28.35 ± 1.31	28.43 ± 0.76	27.11 ± 0.88	>50
12j	15.22 ± 1.19	10.32 ± 0.58	14.55 ± 1.46	16.75 ± 1.20	19.06 ± 0.90	>50
12k	4.06 ± 1.21	3.75 ± 1.07	8.42 ± 1.23	6.28 ± 0.79	5.80 ± 1.63	>50
12l	7.58 ± 0.86	6.71 ± 1.36	8.09 ± 1.05	9.51 ± 1.21	10.74 ± 0.25	>50
1a	4.54 ± 0.43	7.65 ± 0.72	10.98 ± 1.21	9.85 ± 1.08	11.05 ± 1.03	25.05 ± 2.13

^a Each data represents mean ± S.D. from three different experiments performed in triplicate.

human cancer cell lines. In addition, the inhibition activities of compounds **7a-7l** and **12a-12l** against HL-7702 normal cells were also measured. The results are listed in Table 1. Interestingly, all target compounds displayed lower cytotoxicity on human normal liver cell line HL-7702 than compound **1a**. The results indicated that the cytotoxicity of most of compounds against cancer cells was much higher than HL-7702 normal cells, making them have good selectivity against cancer cells.

2.2.2. Antitumor activity of compound **12k** against drug-resistant cancer cell lines

Paclitaxel is used as first-line chemotherapy agent for human non-small-cell lung cancer (A549) and human epithelial cervical cancer (HeLa), while inherent or acquired resistance becomes a major problem. According to the above biological result, we further investigated the sensitivity of compound **12k** against paclitaxel-resistant and the corresponding sensitive cancer cells (A549 and HeLa). As shown in Table 2, the IC₅₀ value of paclitaxel for A549 and HeLa resistant cancer cell lines were increased to 1.51 and 1.53 μM, respectively, compared with those for the corresponding sensitive cancer cells. Interestingly, the activity of compound **12k** did not markedly vary for these two paclitaxel-resistant cancer cells compared with the sensitive ones, with the IC₅₀ value of compound **12k** against paclitaxel-resistant cancer lines A549 and HeLa were increased to 6.25 and 5.95 μM, respectively. Moreover, compound **12k** had a much lower resistance index (1.20 for resistant A549 cells

and 1.31 for resistant HeLa cells) than paclitaxel (158.6 for resistant A549 cells and 186.4 for resistant HeLa cells), respectively.

2.2.3. In vitro tubulin polymerization inhibition activity

It is well-known that microtubule-targeting agents can be divided into two types: microtubule stabilizing agents (e.g., paclitaxel) and microtubule destabilizing agents (e.g., colchicine and CA-4) [36]. In order to further confirm which type of microtubule-targeting agents compounds **7h** and **12k** are, the *in vitro* tubulin polymerization inhibition activities of compounds **7h** and **12k** were investigated. Compounds **7h** and **12k** were employed at respective 15 μM for microtubule dynamics assays with paclitaxel and CA-4 as positive controls, respectively. As illustrated in Fig. 2, paclitaxel (10 μM) was found to stimulate tubulin polymerization, while CA-4 (10 μM) almost completely inhibited tubulin polymerization as expected. For compounds **7h** and **12k**, an obvious inhibition of polymerization was observed. These data indicated that both **7h** and **12k** can effectively inhibit tubulin polymerization and act as potential microtubule destabilizing agents for cancer therapy.

2.2.4. Molecular docking

To determine the possible binding mode of the chalcone derivatives, compounds **7** and **12** were chosen to perform a molecular docking to ensure that the chalcone derivatives have the same binding site as colchicine and compound **4**. The binding modes of **7h**, **12k**, colchicine and **4** in the colchicine binding site of tubulin are

Table 2
In vitro growth inhibitory effect of compound **12k** on paclitaxel-resistant cancer cell lines A549 and HeLa.

Compd.	IC ₅₀ (μM)		resistant factor ^a	IC ₅₀ (μM)		resistant factor ^a
	A549	A549/resistant		HeLa	HeLa/resistant	
12k	5.21 ± 0.45	6.25 ± 0.75	1.20	4.53 ± 0.62	5.95 ± 1.21	1.31
paclitaxel	9.52 ± 2.12 ^b	1.51 ± 0.53	158.6	8.21 ± 3.27 ^b	1.53 ± 0.31	186.4

^a Resistance index = IC₅₀(resistant)/IC₅₀(sensitive).

^b IC₅₀ unit for paclitaxel is nM.

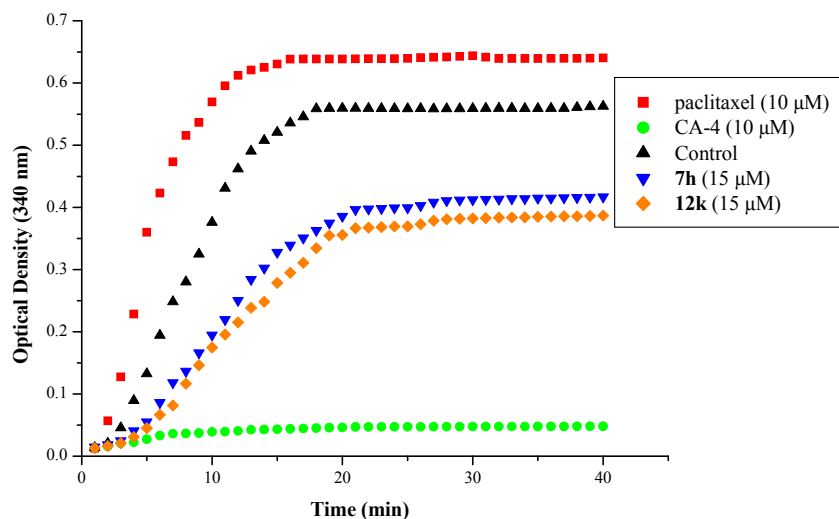


Fig. 2. Effects of compounds **7h** and **12k** on microtubule dynamics. Polymerization of tubulin at 37 °C in the presence of paclitaxel (10 μM), CA-4 (10 μM), compound **7h** (15 μM) and compound **12k** (15 μM) was monitored continuously by recording the absorbance at 340 nm over 40 min. The reaction was initiated by the addition of tubulin to a final concentration of 3.0 mg/mL.

depicted in Fig. 3 and the docking scores obtained are summarized in Table 3. The Surflex docking scores are 12.53 for **7h** and 12.31 for **12k**, where higher scores indicate greater binding affinity. Biological activity studies suggested that compounds **7h** and **12k** potentially inhibited tubulin polymerization, hence, the docking detail of these two compounds were examined to compare with those of 1SA0-colchicine and compound **4** to evaluate binding modes.

Fig. 3A shows that the interacting mode of compound **7h** with chalcone moiety in the binding site is surrounded by Cys241, Leu248, Lys 254, Leu255, Lys352 and Leu354. In particular, compound **7h** forms three hydrogen bonds with the polar amino acids Asn101, suggesting a probable strong electrostatic interaction with the protein. In addition, the hydrophobic moiety of the compound **7h** is well embedded in a pocket interacting with several hydrophobic residues making compound **7h** bind tightly to tubulin. Not surprisingly, the accommodation of compound **12k** in the binding site is also similar to colchicine (Fig. 3B). In this case, docking simulations showed that the 3,4,5-trimethoxy-phenyl ring of compound **12k** like colchicine can also be accommodated in the same hydrophobic groove, adopting an energetically stable conformation. Moreover, the methoxy group, the carbonyl oxygen atom of 3,4,5-trimethoxy-phenyl moiety and the oxygen atom of amide in compound **12k** as acceptors establish three hydrogen bonds with Ser178, Tyr224 and Asn249, respectively, which is consistent with the observation that colchicine stabilizes the tubulin heterodimer and further confirms that this moiety is also crucial for binding (Fig. 3B). Similar interactions with Ser178 or Tyr224 can be observed in the binding mode of compound **4**. It is interesting to note that the crucial electrostatic interactions between the methoxy group of the 3,4,5-trimethoxy-phenyl unit and residues Ser178, Lys254 and Asn101 of the neighboring α -subunit are observed in the binding pocket, demonstrating a plausible competitive mechanism of action at the colchicine site.

2.2.5. Compound **12k** induces apoptosis in NCI-H460

Among all the target compounds, compound **12k** was found to exhibit the best antitumor activity against the NCI-H460 cancer cells, hence, the apoptosis ratios induced by **12k** in NCI-H460 cancer cells were determined by flow cytometry. NCI-H460 cells were co-stained with Annexin-V FITC and PI, and the apoptotic cells were observed by flow cytometric analysis. In Fig. 4, the Q1 area

represents damaged cells, the Q2 region represents necrotic cells and later period apoptotic cells, the Q3 area represents early apoptotic cells, and the Q4 area represents the normal cells, respectively. It was found that compound **12k** could induce apoptosis in NCI-H460 cells. Apoptosis ratios (including the early and late apoptosis ratios cells) were showed after treatment with **12k** for 24 h at the concentration of 5 and 10 μM, respectively. The apoptosis of NCI-H460 cells treatment with the compound increased gradually in a dose-dependent manner. The apoptosis ratios of compound **12k** at two concentrations were found to be 15.35% and 66.4%, respectively, while that of control was only 1.44%. The results evidently manifested that compound **12k** effectively induced apoptosis in NCI-H460 cells in comparison with the control.

2.2.6. Morphological characterization of cell apoptosis of NCI-H460 cells by Hoechst 33258

To further determine whether the observed cell death induced by compound **12k** was due to apoptosis, untreated cells were used as a negative control and NCI-H460 cells treated with different concentrations of compound **12k** for 24 h were stained with Hoechst 33258. As shown in Fig. 5, the control cells displayed weak blue fluorescence, but it was worth noting that the nuclei of NCI-H460 cells appeared hyper-condensed (brightly stained) after treatment with compound **12k** at 5 or 10 μM for 24 h. These results indicated that compound **12k** was able to induce apoptosis in a dose-dependent manner.

2.2.7. Cell cycle analysis

As most anti-mitotic agents display the ability to disrupt the regulated cell cycle distribution, the effect of a 48 h treatment with different concentrations of compound **12k** on cell cycle progression was also evaluated by flow cytometry in NCI-H460 cells. Untreated cells were used as a negative control and NCI-H460 cells were treated with compound **12k** at 5 and 10 μM for 48 h, respectively. The cells were harvested, and the cell cycle phases were examined by flow cytometry. As shown in Fig. 6, G1 period cells gradually decreased and S period cells did not change significantly, while G2 phase cells markedly increased compared with the control group. At 5 μM of compound **12k**, 11.88% of G2 phase was arrested, while the concentration of compound **12k** was increased to 10 μM, 72.44%

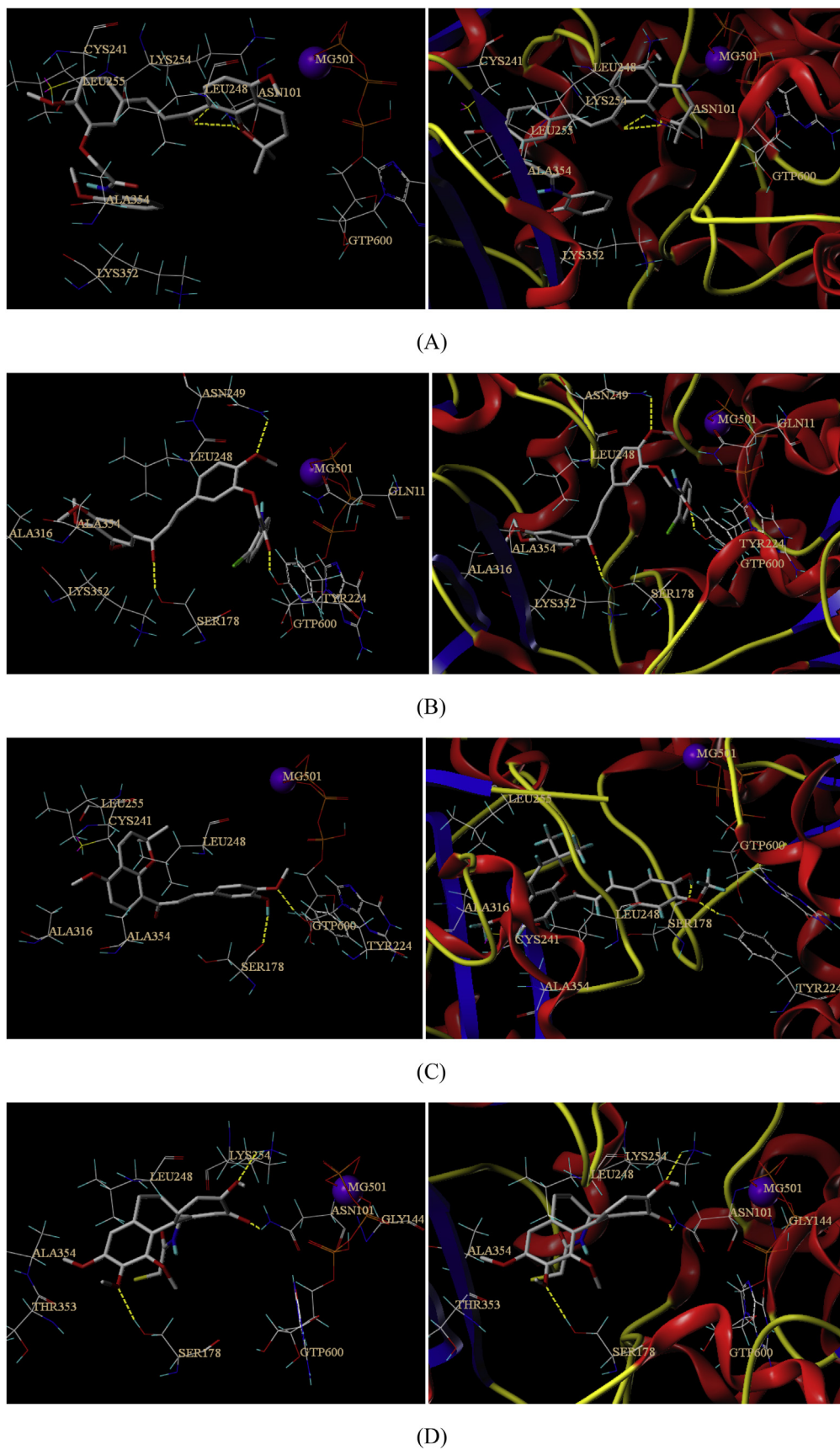


Fig. 3. Molecular modeling of **7h**, **12k**, **4** and 1SA0-colchicine in complex with tubulin. Illustrated are the proposed binding mode and interaction between tubulin and selected compounds, (A) compound **7h**, (B) compound **12k**, (C) **4**, (D) 1SA0-colchicine. The compounds and important amino acids in the binding pockets are shown in stick model, whereas tubulin is depicted in the ribbon model. The Mg^{2+} -ion is shown as a purple sphere. (For interpretation of the references to colour in this figure legend, the reader is referred to the web version of this article.)

G2 phase arrest was observed. These results showed that compound **12k** markedly arrested the G2 phase of the cell cycle in a dose-dependent manner.

2.2.8. Compound **12k** triggers ROS generation

Comprehensive literature indicated that intracellular ROS plays a vital role in the regulation of cell apoptosis [37–39]. Thus, we further investigated whether ROS stimulated by compound **12k** induced apoptosis in NCI-H460 cells. Cells were treated with compound **12k** (5 and 10 μ M) for 24 h using the fluorescent probe 2,7-dichlorofluorescein diacetate (DCF-DA) analysis by flow cytometry with untreated cells as a negative control. As illustrated in Fig. 7, the cells treated with different concentrations of compound **12k** exhibited ROS generation level increased in a dose-dependent manner compared with control cells. In short, these data hinted that compound **12k** caused oxidative imbalance in NCI-H460 cells.

2.2.9. Compound **12k** triggers mitochondrial pathway dependent apoptosis

The loss of mitochondrial membrane potential (MMP) is regarded as an important factor in the apoptotic pathway [40–42]. In order to further evaluate the apoptosis-inducing effect of compound **12k**, MMP changes were detected using the fluorescent probe JC-1. NCI-H460 cells were treated with compound **12k** (5, 10 μ M) for 24 h using untreated cells as a negative control. As shown in Fig. 8, compound **12k** induced a dose-dependent manner increasing in the proportion of cells compared with the control cells, suggesting that compound **12k** treatment induced mitochondrial membrane permeability in NCI-H460 cells. Taken together, these results clearly demonstrated that mitochondrial function is extremely impaired in compound **12k** caused apoptosis in NCI-H460 cells.

2.2.10. Compound **12k** induces apoptosis via the regulation of apoptosis-related protein expression

It is generally accepted that anticancer agents initiated apoptotic signaling through two major pathways [43–45]. One is the death receptor (extrinsic) pathway involving death receptor, and the other is the mitochondrial (intrinsic) pathway. In order to investigate whether compound **12k** induced apoptosis via the mitochondrial signaling pathway, some of major protein markers involved in mitochondria-mediated apoptosis were also analyzed by western blot method. Initially, the level of cytochrome *c* released from the mitochondria to cytosol was evaluated as shown in Fig. 9. Compared with the control, the level of cytochrome *c* in cytosol increased in a dose-dependent manner after treatment with compound **12k** for 48 h. In addition, it has been confirmed that the release of cytochrome *c* can stimulate apoptosis via the mitochondrial pathway by activation of the downstream caspase-9 and caspase-3 [46,47]. Secondly, the roles of caspase-9 and caspase-3 in the cellular response to compound **12k** were further investigated. As illustrated in Fig. 9, western blot analysis displayed that treatment of NCI-H460 cells with compound **12k** effectively induced cleavage of caspase-9 and caspase-3, respectively. Since the Bcl-2 family proteins are critical regulators of the mitochondrial apoptotic pathway, the anti-apoptotic protein Bcl-2 and the pro-apoptotic protein Bax are important regulators of this progress [48,49]. Finally, to confirm the mechanism of compound **12k** induced in NCI-H460 cells apoptosis, the expression of Bax and Bcl-2 proteins was investigated. Western blot analysis exhibited that the protein expression level of Bax effectively increased, while the protein expression level of Bcl-2 significantly decreased in a dose-dependent manner compared with control (Fig. 9).

3. Conclusion

In this investigation, a class of novel chalcone analogues were designed and synthesized, and their cell growth inhibition activities against HepG-2, NCI-H460, MGC-803, SK-OV-3 and T24 cancer cell lines were investigated using MTT assay. The *in vitro* antitumor activities result showed that among these compounds, **12k** exhibited excellent anti-proliferative activities against five human cancer cell lines including multidrug resistant human tumor cell lines. The apoptosis-inducing activity of **12k** in NCI-H460 cells was investigated by Hoechst 33258 staining, JC-1 mitochondrial membrane potential staining, ROS generation assay and flow cytometry. In addition, molecular mechanism studies indicated that compound **12k** was found to induce apoptosis in NCI-H460 cells via the mitochondrial pathway, and the cell cycle analysis suggested that compound **12k** significantly induced cell cycle arrest in G2/M phase. Moreover, the results of tubulin polymerization assay displayed that the novel chalcone analogues could inhibit tubulin polymerization, and molecular docking analysis indicated that **12k** can be binding to the colchicine site of tubulin. Taken together, these results suggested that compound **12k** is a promising anti-tumor agent to inhibit tubulin polymerization.

4. Experimental

All chemicals and solvents were of analytical reagent grade and provided by Energy Chemical, Shanghai of China and used without further purification, unless noted specifically. Column chromatography was performed using silica gel (200–300 mesh). ^1H NMR and ^{13}C NMR spectra were recorded in CDCl_3 or $\text{DMSO}-d_6$ with a Bruker 300 or 400 MHz spectrometer. Mass spectra were measured on an Agilent 6224 TOF LC/MS instrument.

4.1. General procedure for the preparation of compounds **7a–7l** and **12a–12k**

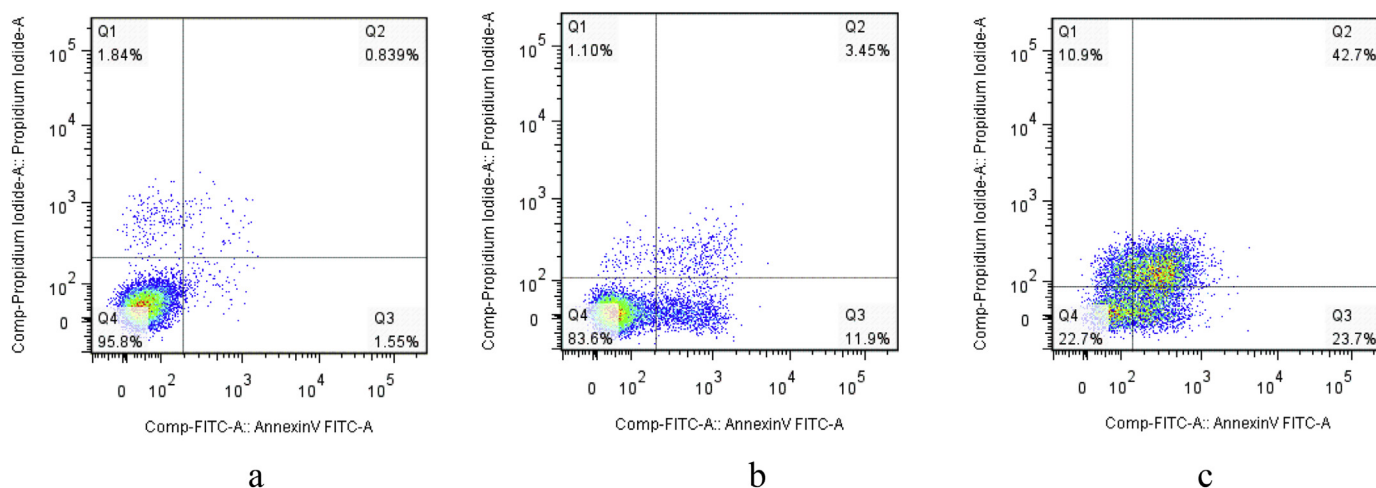
Synthesis of compound **2**. To a solution of compound **1** (2.32 g, 20.0 mmol) in dry CH_3CN (150 mL), DBU (3.0 mL, 30.0 mmol), $\text{CuCl}_2 \cdot 2\text{H}_2\text{O}$ (10 mg, 0.6 mmol), and 3-chloro-3-methyl-1-butene (3.06 g, 30.0 mmol) were added at 0 $^\circ\text{C}$. The mixture was stirred at the same temperature for 12 h, then 1 N HCl (aq) was added to adjust pH = 2. After the solvent was removed under reduced pressure, the residue was poured into water (50 mL) to yield yellow precipitate that was collected by filtration and washed with petroleum ether to produce compound **2** as a yellow solid (yield, 3.5 g, 76.1%) which was used directly without further purification. ^1H NMR (300 MHz, CDCl_3) δ 7.75 (d, J = 8.8 Hz, 1H, ArH), 7.18 (s, 1H, ArH), 6.59 (d, J = 8.8 Hz, 1H, ArH), 3.83 (s, 3H, $-\text{OCH}_3$), 2.67 (s, 1H, $-\text{C}\equiv\text{CH}$), 2.57 (s, 3H, $-\text{CH}_3$), 1.74 (s, 6H, $2 \times -\text{CH}_3$). HR-MS (m/z) (ESI): calcd for $\text{C}_{14}\text{H}_{18}\text{O}_3$ [$\text{M}+\text{H}^+$]: 233.11777; found: 233.11902.

Synthesis of compound **3**. A solution of compound **2** (2.32 g, 10.0 mmol) in dry pyridine (50 mL) was stirred at 120 $^\circ\text{C}$, which was monitored by TLC. After completion of reaction for 12 h, the mixture was concentrated under reduced pressure, the resulting crude product was purified by chromatography on silica gel eluted with petroleum ether/ethyl acetate (V:V = 50:1) to offer compound **3** as a yellow oil (yield: 1.7 g, 73.3%). ^1H NMR (300 MHz, CDCl_3) δ 7.74 (d, J = 8.9 Hz, 1H, ArH), 6.67 (d, J = 10.0 Hz, 1H, ArH), 6.47 (d, J = 8.9 Hz, 1H, Ph- $\text{CH}=\text{CH}-\text{C}(\text{CH}_3)_2$), 5.61 (d, J = 10.0 Hz, 1H, Ph- $\text{CH}=\text{CH}-\text{C}(\text{CH}_3)_2$), 3.86 (s, 3H, $-\text{OCH}_3$), 2.61 (s, 3H, $-\text{CH}_3$), 1.49 (s, 6H, $2 \times -\text{CH}_3$). HR-MS (m/z) (ESI): calcd for $\text{C}_{14}\text{H}_{18}\text{O}_3$ [$\text{M}+\text{H}^+$]: 233.11777; found: 233.11738.

Synthesis of compound **4**. A solution of 50% KOH (15 mL, aq) was added dropwise to a stirred solution of compound **3** (1.5 g, 6.46 mmol) and 3-hydroxy-4-methoxybenzaldehyde (0.98 g,

Table 3
Docking scores (kcal/mol) for all studied compounds.

Compd.	Score	Crash	Polar	D-Score	PMF Score	G-Score	Chem-Score	CScore
7a	9.71	-1.83	2.03	-174.40	-3.78	-312.00	-34.86	5
7b	11.70	-1.21	0.00	-172.50	-18.61	-323.81	-32.49	5
7c	10.97	-0.83	1.23	-158.68	-9.53	-299.31	-32.66	4
7d	9.35	-1.63	0.51	-179.63	-8.42	-336.89	-32.72	4
7e	9.64	-1.72	0.32	-171.05	-4.01	-350.42	-33.15	5
7f	10.09	-1.03	0.00	-174.90	-7.01	-325.39	-33.77	5
7g	9.68	-1.57	2.01	-160.68	-4.79	-304.02	-30.13	3
7h	12.53	-1.72	1.70	-192.69	3.20	-372.87	-33.69	4
7i	10.39	-1.59	0.73	-167.89	7.65	-322.27	-31.50	3
7j	9.20	-2.54	1.99	-171.21	9.13	-292.28	-33.27	3
7k	10.02	-2.01	2.49	-169.44	-1.46	-296.49	-31.04	2
7l	9.89	-2.12	0.96	-176.91	-1.21	-300.44	-28.30	4
12a	10.53	-2.44	0.57	-167.74	2.94	-300.44	-31.63	4
12b	11.13	-2.86	1.22	-181.67	8.95	-308.39	-28.82	4
12c	10.61	-2.06	2.05	-165.12	-32.29	-296.47	-33.16	5
12d	10.95	-0.80	2.77	-150.24	-24.89	-253.22	-25.60	2
12e	9.07	-3.16	2.02	-170.86	-6.81	-287.92	-28.38	3
12f	9.10	-1.51	2.44	-167.71	-6.95	-264.87	-28.11	3
12g	7.88	-2.03	1.05	-152.99	-10.91	-260.31	-26.46	4
12h	10.64	-4.44	2.34	-199.87	16.05	-285.07	-37.64	4
12i	9.08	-2.04	1.44	-162.47	-19.06	-269.44	-31.07	5
12j	10.39	-2.66	1.14	-179.89	-17.67	-312.04	-31.52	5
12k	12.31	-1.44	1.43	-181.13	5.59	-326.22	-25.04	3
12l	11.65	-1.65	2.50	-173.01	7.56	-289.46	-27.49	3
4	8.6	0.61	3.09	-120.99	-23.37	-181.69	-228.86	3
colchicine	9.73	-1.34	1.95	-145.65	2.87	-229.93	-21.31	2

**Fig. 4.** Apoptosis ratio detection of compound **12k** by Annexin V/PI assay. (a) Untreated NCI-H460 cells as control for 24 h, (b) treated NCI-H460 cells at 5 μM for 24 h, (c) treated NCI-H460 cells at 10 μM for 24 h.

6.46 mmol) in methanol (30 mL) at 0 °C. The resulting mixture was stirred at the same temperature for 12 h and monitored by TLC. After completion of reaction, the mixture was poured into ice-water and adjusted to pH = 2 with 4 N HCl. The precipitated was filtered, washed with water and dried to offer the crude product which was purified by chromatography on silica gel eluted with petroleum ether/ethyl acetate (V:V = 3:1, 2:1) to give the desired compound as a yellow solid (yield: 1.5 g, 65.2%). $^1\text{H NMR}$ (300 MHz, CDCl_3) δ 7.70 (d, J = 8.8 Hz, 1H, ArH), 7.66–7.53 (m, 2H, ArH), 7.21 (d, J = 1.7 Hz, 1H, ArH), 7.11–7.08 (m, 1H, ArH), 6.86 (d, J = 8.3 Hz, 1H, Ph-CO-CH=CH-), 6.69 (d, J = 10.0 Hz, 1H, Ph-CO-CH=CH-), 6.51 (d, J = 8.8 Hz, 1H, Ph-CH=CH-C(CH₃)₂), 5.68 (s, 1H, -OH), 5.63 (d, J = 10.0 Hz, 1H, Ph-CH=CH-C(CH₃)₂), 3.93 (s, 3H, -OCH₃), 3.88 (s, 3H, -OCH₃), 1.51 (s, 6H, 2 \times -CH₃). HR-MS (m/z) (ESI): calcd for $\text{C}_{14}\text{H}_{22}\text{O}_5$ [$\text{M}+\text{H}^+$]: 367.15455; found: 367.15061.

Synthesis of compound **5**. To a solution of compound **4** (1.83 g,

5.0 mmol) in DMF (15 mL), α -bromoethyl acetate (1.09 g, 6.5 mmol), K_2CO_3 (695 mg, 10.0 mmol) and KI (85 mg, 0.5 mmol) were added. The mixture was stirred overnight at room temperature. Then the mixture was diluted with water (250 mL) and extracted with CH_2Cl_2 (2 \times 150 mL). The organic phase was dried over anhydrous Na_2SO_4 and concentrated under reduced pressure. The residue was purified by chromatography on silica gel eluted with petroleum ether/ethyl acetate (V:V = 1.5:1) to offer the desired product as a yellow oil (yield: 2.1 g, 93.3%). $^1\text{H NMR}$ (300 MHz, CDCl_3) δ 7.69 (d, J = 8.8 Hz, 1H, ArH), 7.64–7.50 (m, 2H, ArH), 7.23 (s, 1H, ArH), 7.09 (d, J = 1.5 Hz, 1H, ArH), 6.91 (d, J = 8.4 Hz, 1H, Ph-CO-CH=CH-), 6.69 (d, J = 10.0 Hz, 1H, Ph-CO-CH=CH-), 6.51 (d, J = 8.9 Hz, 1H, Ph-CH=CH-C(CH₃)₂), 5.62 (d, J = 10.0 Hz, 1H, Ph-CH=CH-C(CH₃)₂), 4.69 (s, 2H, -O-CH₂-COOCH₂CH₃), 4.26 (q, J = 7.1 Hz, 2H, -CH₂CH₃), 3.91 (s, 3H, -OCH₃), 3.87 (s, 3H, -OCH₃), 1.50 (s, 6H, 2 \times -CH₃), 1.28 (t, J = 7.2 Hz, 3H, -CH₂CH₃). HR-MS (m/z) (ESI): calcd for $\text{C}_{26}\text{H}_{28}\text{O}_7$

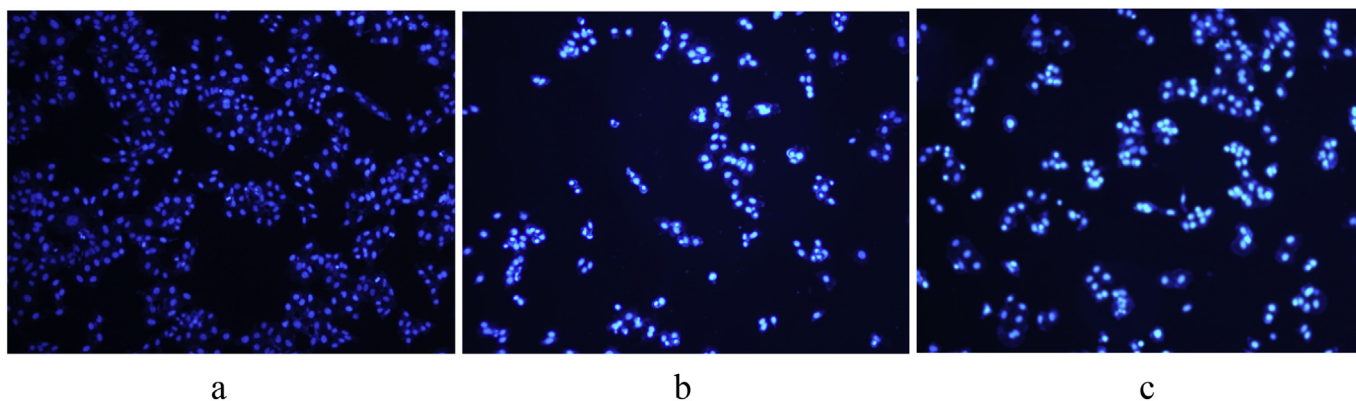


Fig. 5. Hoechst 33258 staining of compound **12k** in NCI-H460 cells. (a) Untreated NCI-H460 cells were used as control at for 24 h and (b, c) NCI-H460 cells were treated with compound **12k** at 5 and 10 μM for 24 h, respectively.

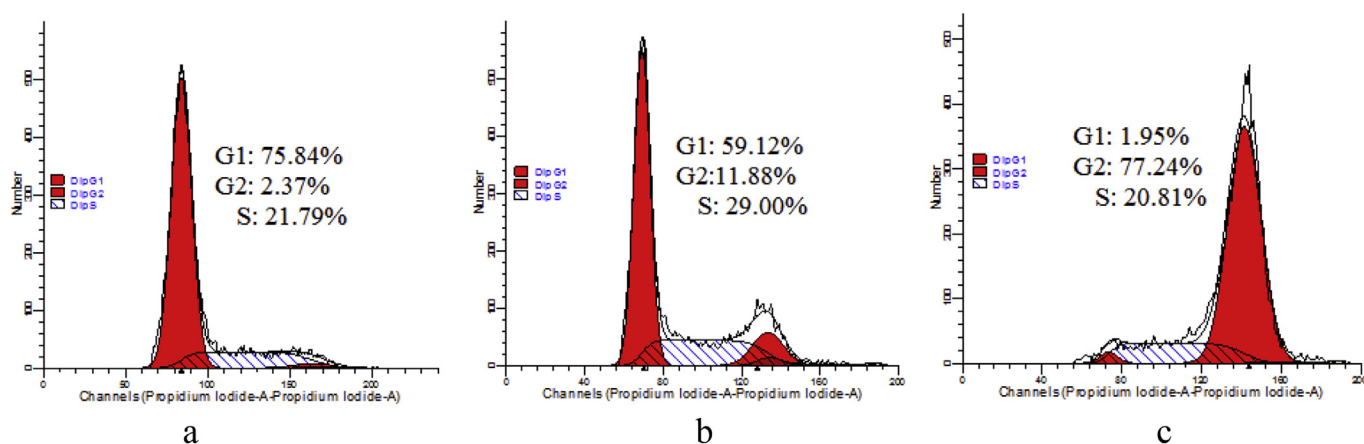


Fig. 6. Investigation of cell cycle distribution by flow cytometric analysis. (a) Untreated NCI-H460 cells as a control. (b) and (c) NCI-H460 cells were treated with increasing concentrations of compound **12k** (5 and 10 μM) for 48 h, respectively.

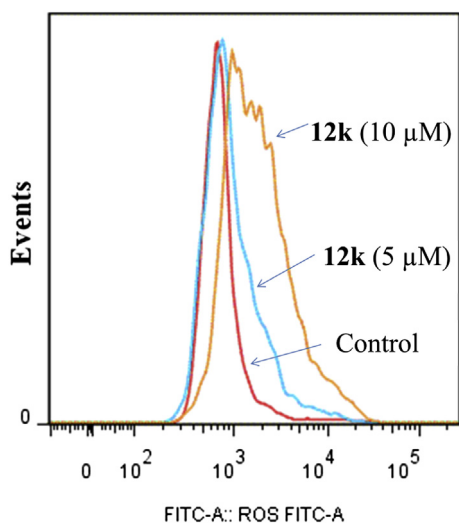


Fig. 7. ROS generation assay of compound **12k** in NCI-H460 cells after treatment with 5 and 10 μM for 24 h.

$[\text{M}+\text{H}^+]$: 453.19133; found:453.18403.

Synthesis of compound 6. To a solution of compound **5** (3.6 g, 7.96 mmol) in THF/H₂O (50/10 mL) lithium hydroxide (1.33 g,

31.8 mmol) was added and stirred at room temperature for 2 h. After the reaction mixture was adjusted pH = 2 with 1 N HCl solution, 150 mL of water was added. The solution was extracted with CH₂Cl₂ (2 × 100 mL), then the organic phase was dried over anhydrous Na₂SO₄ and concentrated under reduced pressure to obtain the target product as a yellow solid (yield: 3.2 g, 95.0%). ¹H NMR (300 MHz, CDCl₃) δ 7.69 (d, *J* = 8.8 Hz, 1H, ArH), 7.64–7.49 (m, 2H, ArH), 7.22 (s, 1H, ArH), 7.12 (s, 1H, ArH), 6.88 (d, *J* = 8.3 Hz, 1H, Ph-CO-CH=CH-), 6.67 (d, *J* = 10.1 Hz, 1H, Ph-CO-CH=CH-), 6.50 (d, *J* = 8.8 Hz, 1H, Ph-CH=CH-C(CH₃)₂), 5.61 (d, *J* = 10.0 Hz, 1H, Ph-CH=CH-C(CH₃)₂), 4.66 (s, 2H, -O-CH₂-COOH), 3.87 (s, 6H, 2 × -OCH₃), 1.48 (s, 6H, 2 × -CH₃). HR-MS (*m/z*) (ESI): calcd for C₂₄H₂₄O₇ [$\text{M}+\text{H}^+$]: 425.16003; found: 425.14932.

Synthesis of compound 9. A solution of 50% KOH (15 mL, aq) was added dropwise to a stirred solution of compound **8** (1.5 g, 7.14 mmol) and 3-hydroxy-4-methoxybenzaldehyde (1.09 g, 7.14 mmol) in methanol (25 mL) at 0 °C. The resulting mixture was stirred at the same temperature for 12 h and monitored by TLC. After completion of reaction, the mixture was poured into ice-water and adjusted to pH = 2 with 4 N HCl. The deposit was filtered, washed with water and dried to offer the crude product, which was purified by chromatography on silica gel eluted with petroleum ether/ethyl acetate (V:V = 4:1, 3:1, 2:1) to give the desired compound as a yellow solid (yield: 2.3 g, 54.8%). ¹H NMR (300 MHz, DMSO-*d*₆) δ 9.13 (s, 1H, ArH), 7.73–7.59 (m, 2H, ArH), 7.40 (s, 2H, ArH), 7.37 (s, 1H, -OH), 7.30 (d, *J* = 8.4 Hz, 1H, Ph-CO-

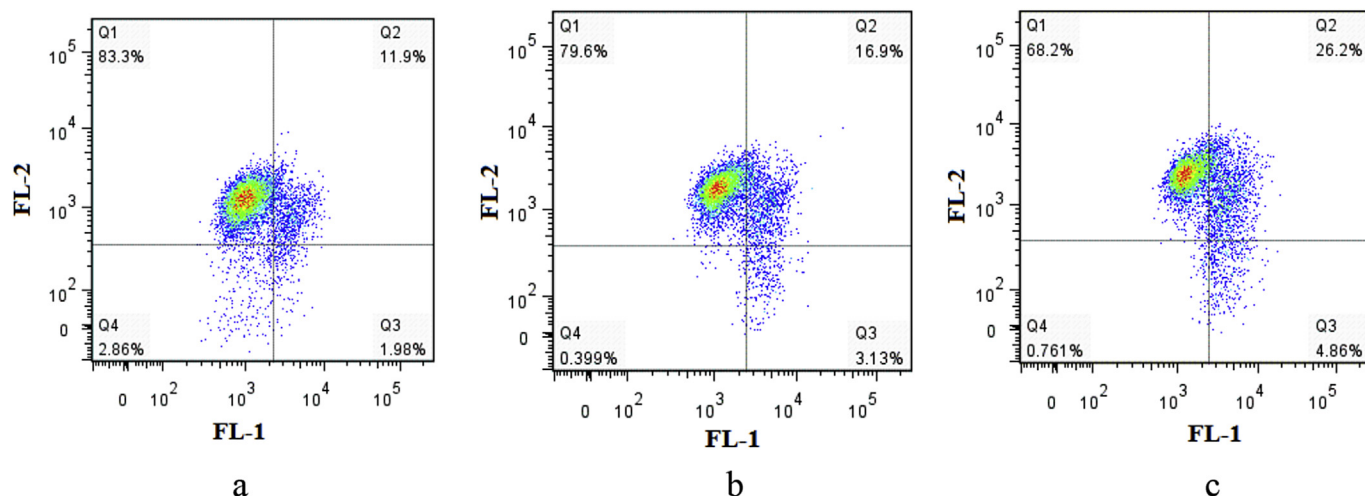


Fig. 8. JC-1 mitochondrial membrane potential staining of compound **12k** in NCI-H460 cells. (a) Untreated cells as control for 24 h and (b, c) treated cells with compound **12k** at 5 and 10 μM for 24 h, respectively.

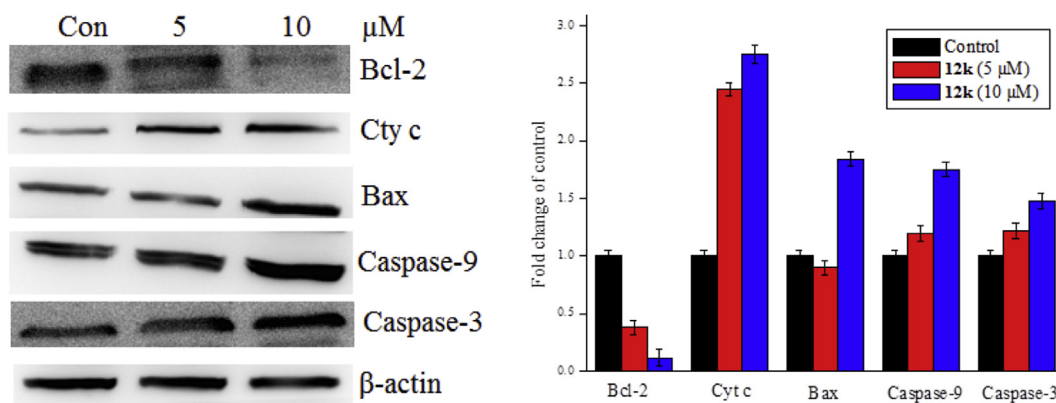


Fig. 9. Western blot analysis of Cyt c, Bax, Bcl-2, caspase-9 and caspase-3 after treatment of NCI-H460 cells with compound **12k** at the indicated concentrations and for the indicated times. β -actin antibody was used as reference control.

$\text{CH}=\text{CH}-$), 7.00 (d, $J = 8.3$ Hz, 1H, $\text{Ph-CO-CH}=\text{CH}-$), 3.90 (s, 6H, $2 \times -\text{OCH}_3$), 3.84 (s, 3H, $-\text{OCH}_3$), 3.76 (s, 3H, $-\text{OCH}_3$). HR-MS (m/z) (ESI): calcd for $\text{C}_{19}\text{H}_{20}\text{O}_6$ [$\text{M}+\text{H}^+$]: 345.13381; found: 345.13371.

Synthesis of compound 10. To a solution of compound **9** (1.75 g, 5.1 mmol) in DMF (15 mL), α -bromoethyl acetate (1.02 g, 6.1 mmol), K_2CO_3 (1.4 g, 10.2 mmol) and KI (85 mg, 0.51 mmol) were added. The mixture was stirred overnight at room temperature, then it was diluted with water (300 mL) and extracted with CH_2Cl_2 (2×150 mL). The organic phase was dried over anhydrous Na_2SO_4 and concentrated under reduced pressure. The residue was purified by chromatography on silica gel eluted with petroleum ether/ethyl acetate (V:V = 1.5:1) to offer the desired product as a yellow solid (yield: 2.0 g, 90.9%). ^1H NMR (300 MHz, CDCl_3) δ 7.80 (d, $J = 15.5$ Hz, 1H, ArH), 7.41–7.38 (m, 2H, ArH), 7.34 (s, 2H, ArH), 7.25 (d, $J = 8.6$ Hz, 1H, $\text{Ph-CO-CH}=\text{CH}-$), 7.02 (d, $J = 8.3$ Hz, 1H, $\text{Ph-CO-CH}=\text{CH}-$), 4.81 (s, 2H, $-\text{O-CH}_2\text{-COOCH}_2\text{CH}_3$), 4.41–4.33 (m, 2H, $-\text{CH}_2\text{CH}_3$), 4.03 (d, $J = 6.5$ Hz, 12H, $4 \times -\text{OCH}_3$), 1.38 (t, $J = 7.1$ Hz, 3H, $-\text{CH}_2\text{CH}_3$). HR-MS (m/z) (ESI): calcd for $\text{C}_{23}\text{H}_{26}\text{O}_8$ [$\text{M}+\text{H}^+$]: 431.17059; found: 431.16823.

Synthesis of compound 11. To a solution of compound **10** (2.0 g, 4.65 mmol) in THF/ H_2O (30/5 mL) lithium hydroxide (979 mg, 23.3 mmol) was added and stirred at room temperature for 2 h. The reaction mixture was adjusted pH = 2 with 1 N HCl solution, then 150 mL of water was added. The resulting aqueous solution was

extracted with CH_2Cl_2 (2×100 mL), the organic phase was dried over anhydrous Na_2SO_4 and concentrated under reduced pressure to obtain the target product as a yellow solid (yield: 1.7 g, 91.9%). ^1H NMR (300 MHz, $\text{DMSO}-d_6$) δ 12.97 (s, 1H, $-\text{COOH}$), 7.76 (d, $J = 15.5$ Hz, 1H, ArH), 7.67 (d, $J = 15.5$ Hz, 1H, ArH), 7.54–7.43 (m, 2H, ArH, $\text{Ph-CO-CH}=\text{CH}-$, overlapped signals), 7.39 (s, 2H, ArH), 7.07 (d, $J = 8.4$ Hz, 1H, $\text{Ph-CO-CH}=\text{CH}-$), 4.78 (s, 2H, $-\text{O-CH}_2\text{-COOH}$), 3.90 (s, 6H, $2 \times -\text{OCH}_3$), 3.85 (s, 3H, $-\text{OCH}_3$), 3.77 (s, 3H, $-\text{OCH}_3$). HR-MS (m/z) (ESI): calcd for $\text{C}_{21}\text{H}_{22}\text{O}_8$ [$\text{M}-\text{H}^+$]: 401.12364; found: 401.12445.

Synthesis of compounds 7a–7l. To a solution of compound **6** (150 mg, 0.353 mmol), EDCI (104 mg, 0.530 mmol) and HOBT (72 mg, 0.530 mmol) in dry DMF (3 mL), anilines (0.353 mmol) was added. After the mixture was stirred overnight at room temperature, it was diluted with water (250 mL) and extracted with CH_2Cl_2 (100 mL). The organic phase was dried over anhydrous Na_2SO_4 and concentrated under reduced pressure. The residue was purified by chromatography on silica gel eluted with petroleum ether/ethyl acetate (V:V = 6:1, 3:1) to offer the desired products as yellow solids.

Synthesis of compounds 12a–12k. To a solution of compound **11** (130 mg, 0.323 mmol), EDCI (93 mg, 0.485 mmol) and HOBT (65 mg, 0.485 mmol) in dry DMF (3 mL), anilines (0.323 mmol) was added in reaction. The mixture was stirred overnight at room temperature, then it was diluted with water (300 mL) and extracted

with CH_2Cl_2 (100 mL). The organic phase was dried over anhydrous Na_2SO_4 and concentrated under reduced pressure. The residue was purified by chromatography on silica gel eluted with petroleum ether/ethyl acetate (V:V = 8:1, 5:1) to offer the desired products as yellow solids.

Compound 7a: yield, 95.2%; ^1H NMR (400 MHz, CDCl_3) δ 8.87 (s, 1H, -CO-NH-), 7.71 (d, J = 8.8 Hz, 1H, ArH), 7.62–7.60 (m, 4H, ArH), 7.35 (t, J = 7.8 Hz, 2H, ArH), 7.30–7.24 (m, 2H, ArH), 7.14 (t, J = 7.4 Hz, 1H, ArH), 6.96 (d, J = 8.4 Hz, 1H, Ph-CO-CH=CH-), 6.70 (d, J = 10.0 Hz, 1H, Ph-CO-CH=CH-), 6.51 (d, J = 8.9 Hz, 1H, Ph-CH=CH-C(CH₃)₂), 5.63 (d, J = 10.0 Hz, 1H, Ph-CH=CH-C(CH₃)₂), 4.66 (s, 2H, -O-CH₂-CO-NH-), 3.97 (s, 3H, -OCH₃), 3.87 (s, 3H, -OCH₃), 1.50 (s, 6H, 2 × -CH₃). ^{13}C NMR (100 MHz, CDCl_3) δ 189.62, 166.39, 158.47, 153.66, 151.45, 147.49, 140.37, 137.22, 131.71, 129.31, 129.10, 128.61, 126.27, 124.85, 124.68, 121.63, 119.87, 116.82, 115.05, 112.13, 110.49, 103.55, 70.28, 56.11, 55.81, 28.10. HR-MS (m/z) (ESI): calcd for $\text{C}_{33}\text{H}_{29}\text{O}_6\text{N}$ [$\text{M}+\text{H}^+$]: 500.20731; found: 500.19839.

Compound 7b: yield, 91.5%; ^1H NMR (400 MHz, CDCl_3) δ 8.74 (s, 1H, -CO-NH-), 7.71 (d, J = 8.8 Hz, 1H, ArH), 7.61 (s, 2H, ArH), 7.55–7.48 (m, 2H, ArH), 7.30–7.25 (m, 1H, ArH), 7.24 (d, J = 1.9 Hz, 1H, ArH), 6.96 (d, J = 8.4 Hz, 1H, ArH), 6.97–6.88 (m, 2H, ArH, Ph-CO-CH=CH-, overlapped signals), 6.70 (d, J = 10.0 Hz, 1H, Ph-CO-CH=CH-), 6.51 (d, J = 8.9 Hz, 1H, Ph-CH=CH-C(CH₃)₂), 5.63 (d, J = 10.0 Hz, 1H, Ph-CH=CH-C(CH₃)₂), 4.65 (s, 2H, -O-CH₂-CO-NH-), 3.96 (s, 3H, -OCH₃), 3.88 (s, 3H, -OCH₃), 3.80 (s, 3H, -OCH₃), 1.50 (s, 6H, 2 × -CH₃). ^{13}C NMR (100 MHz, CDCl_3) δ 189.64, 166.10, 158.46, 156.68, 153.66, 151.43, 147.49, 140.40, 131.70, 130.33, 129.30, 128.61, 126.25, 124.78, 121.63, 116.81, 114.92, 114.25, 112.10, 110.49, 103.54, 70.18, 56.09, 55.81, 55.50, 28.10. HR-MS (m/z) (ESI): calcd for $\text{C}_{31}\text{H}_{31}\text{O}_7\text{N}$ [$\text{M}+\text{H}^+$]: 530.21788; found: 530.21028.

Compound 7c: yield, 94.5%; ^1H NMR (400 MHz, CDCl_3) δ 8.79 (s, 1H, -CO-NH-), 7.71 (d, J = 8.8 Hz, 1H, ArH), 7.61 (s, 2H, ArH), 7.49–7.47 (m, 2H, ArH), 7.31–7.22 (m, 2H, ArH), 7.15 (d, J = 8.2 Hz, 2H, ArH), 6.96 (d, J = 8.4 Hz, 1H, Ph-CO-CH=CH-), 6.70 (d, J = 10.0 Hz, 1H, Ph-CO-CH=CH-), 6.51 (d, J = 8.9 Hz, 1H, Ph-CH=CH-C(CH₃)₂), 5.63 (d, J = 10.0 Hz, 1H, Ph-CH=CH-C(CH₃)₂), 4.65 (s, 2H, -O-CH₂-CO-NH-), 3.97 (s, 3H, -OCH₃), 3.88 (s, 3H, -OCH₃), 2.33 (s, 3H, -CH₃), 1.50 (s, 6H, 2 × -CH₃). ^{13}C NMR (100 MHz, CDCl_3) δ 189.65, 166.20, 158.46, 153.66, 151.45, 147.51, 140.39, 134.65, 134.32, 131.71, 129.58, 129.31, 128.61, 126.26, 124.83, 121.65, 119.92, 116.81, 115.00, 112.10, 110.49, 103.54, 70.26, 56.10, 55.81, 28.10, 20.91. HR-MS (m/z) (ESI): calcd for $\text{C}_{31}\text{H}_{31}\text{O}_6\text{N}$ [$\text{M}+\text{H}^+$]: 514.22296; found: 514.21420.

Compound 7d: yield, 90.6%; ^1H NMR (400 MHz, CDCl_3) δ 8.82 (s, 1H, -CO-NH-), 7.63 (d, J = 8.8 Hz, 1H, ArH), 7.53 (s, 2H, ArH), 7.45–7.42 (m, 2H, ArH), 7.40–7.37 (m, 2H, ArH), 7.23–7.21 (m, 1H, ArH), 7.15 (d, J = 1.9 Hz, 1H, ArH), 6.89 (d, J = 8.4 Hz, 1H, Ph-CO-CH=CH-), 6.62 (d, J = 10.0 Hz, 1H, Ph-CO-CH=CH-), 6.44 (d, J = 8.9 Hz, 1H, Ph-CH=CH-C(CH₃)₂), 5.56 (d, J = 10.0 Hz, 1H, Ph-CH=CH-C(CH₃)₂), 4.57 (s, 2H, -O-CH₂-CO-NH-), 3.89 (s, 3H, -OCH₃), 3.80 (s, 3H, -OCH₃), 1.42 (s, 6H, 2 × -CH₃). ^{13}C NMR (100 MHz, CDCl_3) δ 189.62, 166.48, 158.49, 153.66, 151.38, 147.38, 140.28, 136.32, 132.08, 131.72, 129.38, 128.59, 126.34, 124.89, 121.60, 121.38, 117.27, 116.83, 115.24, 112.18, 110.49, 103.56, 70.30, 56.14, 55.82, 28.10. HR-MS (m/z) (ESI): calcd for $\text{C}_{30}\text{H}_{28}\text{O}_6\text{NBr}$ [$\text{M}+\text{Na}^+$]: 602.09772; found: 602.08574.

Compound 7e: yield, 95.2%; ^1H NMR (400 MHz, CDCl_3) δ 8.89 (s, 1H, -CO-NH-), 7.71 (d, J = 8.8 Hz, 1H, ArH), 7.61 (s, 2H, ArH), 7.57 (d, J = 8.7 Hz, 2H, ArH), 7.33–7.23 (m, 4H, ArH), 6.97 (d, J = 8.4 Hz, 1H, Ph-CO-CH=CH-), 6.70 (d, J = 10.0 Hz, 1H, Ph-CO-CH=CH-), 6.52 (d, J = 8.8 Hz, 1H, Ph-CH=CH-C(CH₃)₂), 5.63 (d, J = 10.0 Hz, 1H, Ph-CH=CH-C(CH₃)₂), 4.65 (s, 2H, -O-CH₂-CO-NH-), 3.97 (s, 3H, -OCH₃), 3.88 (s, 3H, -OCH₃), 1.50 (s, 6H, 2 × -CH₃). ^{13}C NMR (100 MHz, CDCl_3) δ 189.61, 166.46, 158.49, 153.66, 151.38, 147.40, 140.27, 135.81, 131.72, 129.66, 129.39, 129.13, 128.59, 126.35, 124.89, 121.61, 121.05,

116.83, 115.23, 112.18, 110.49, 103.56, 70.29, 56.14, 55.82, 28.10. HR-MS (m/z) (ESI): calcd for $\text{C}_{30}\text{H}_{28}\text{O}_6\text{NCl}$ [$\text{M}+\text{H}^+$]: 534.16834; found: 534.15679.

Compound 7f: yield, 93.1%; ^1H NMR (400 MHz, CDCl_3) δ 8.86 (s, 1H, -CO-NH-), 7.71 (d, J = 8.8 Hz, 1H, ArH), 7.61 (s, 2H, ArH), 7.59–7.56 (m, 2H, ArH), 7.31–7.24 (m, 2H, ArH), 7.05 (t, J = 8.6 Hz, 2H, ArH), 6.97 (d, J = 8.4 Hz, 1H, Ph-CO-CH=CH-), 6.70 (d, J = 10.0 Hz, 1H, Ph-CO-CH=CH-), 6.52 (d, J = 8.8 Hz, 1H, Ph-CH=CH-C(CH₃)₂), 5.63 (d, J = 10.0 Hz, 1H, Ph-CH=CH-C(CH₃)₂), 4.65 (s, 2H, -O-CH₂-CO-NH-), 3.97 (s, 3H, -OCH₃), 3.88 (s, 3H, -OCH₃), 1.50 (s, 6H, 2 × -CH₃). ^{13}C NMR (100 MHz, CDCl_3) δ 189.62, 166.36, 160.79, 158.48, 158.36, 153.66, 151.39, 147.42, 140.31, 133.27, 133.24, 131.72, 129.36, 128.59, 126.32, 124.84, 121.66, 121.61, 121.58, 116.83, 115.87, 115.65, 115.11, 112.16, 110.49, 103.56, 70.21, 56.13, 55.82, 28.09. HR-MS (m/z) (ESI): calcd for $\text{C}_{30}\text{H}_{28}\text{O}_6\text{NF}$ [$\text{M}+\text{H}^+$]: 518.19789; found: 518.18735.

Compound 7g: yield, 85.9%; ^1H NMR (400 MHz, CDCl_3) δ 8.76 (s, 1H, -CO-NH-), 7.71 (d, J = 8.8 Hz, 1H, ArH), 7.61 (s, 2H, ArH), 7.41 (d, J = 8.8 Hz, 2H, ArH), 7.30–7.21 (m, 2H, ArH), 6.96 (d, J = 8.4 Hz, 1H, ArH), 6.83 (d, J = 8.8 Hz, 2H, ArH, Ph-CO-CH=CH-, overlapped signals), 6.69 (d, J = 10.0 Hz, 1H, Ph-CO-CH=CH-), 6.52 (d, J = 8.9 Hz, 1H, Ph-CH=CH-C(CH₃)₂), 5.63 (d, J = 10.0 Hz, 1H, Ph-CH=CH-C(CH₃)₂), 4.64 (s, 2H, -O-CH₂-CO-NH-), 3.95 (s, 3H, -OCH₃), 3.88 (s, 3H, -OCH₃), 1.50 (s, 6H, 2 × -CH₃). ^{13}C NMR (100 MHz, CDCl_3) δ 190.00, 166.45, 158.55, 153.75, 153.43, 151.44, 147.44, 140.70, 131.73, 129.72, 129.24, 128.64, 126.20, 124.75, 122.15, 121.54, 116.78, 115.86, 115.02, 112.12, 110.51, 103.58, 70.08, 56.11, 55.82, 28.10. HR-MS (m/z) (ESI): calcd for $\text{C}_{30}\text{H}_{29}\text{O}_7\text{N}$ [$\text{M}+\text{Na}^+$]: 538.18417; found: 538.1773.

Compound 7h: yield, 89.0%; ^1H NMR (400 MHz, CDCl_3) δ 9.25 (s, 1H, -CO-NH-), 8.41 (d, J = 8.0 Hz, 1H, ArH), 7.71 (d, J = 8.8 Hz, 1H, ArH), 7.61 (s, 2H), 7.29–7.26 (m, 1H, ArH), 7.23 (d, J = 1.9 Hz, 1H, ArH), 7.10–7.06 (m, 1H, ArH), 7.00–6.89 (m, 3H, ArH, Ph-CO-CH=CH-, overlapped signals), 6.69 (d, J = 10.0 Hz, 1H, Ph-CO-CH=CH-), 6.51 (d, J = 8.9 Hz, 1H, Ph-CH=CH-C(CH₃)₂), 5.62 (d, J = 10.0 Hz, 1H, Ph-CH=CH-C(CH₃)₂), 4.65 (s, 2H, -O-CH₂-CO-NH-), 3.95 (s, 3H, -OCH₃), 3.90 (s, 3H, -OCH₃), 3.87 (s, 3H, -OCH₃), 1.49 (s, 6H, 2 × -CH₃). ^{13}C NMR (100 MHz, CDCl_3) δ 189.70, 166.05, 158.43, 153.64, 151.58, 148.43, 147.28, 140.63, 131.68, 129.00, 128.64, 126.96, 126.06, 124.59, 124.32, 121.69, 121.10, 120.09, 116.80, 113.98, 112.10, 110.49, 110.24, 103.52, 69.48, 56.06, 55.88, 55.80, 28.06. HR-MS (m/z) (ESI): calcd for $\text{C}_{31}\text{H}_{31}\text{O}_7\text{N}$ [$\text{M}+\text{H}^+$]: 530.21788; found: 530.20973.

Compound 7i: yield, 82.5%; ^1H NMR (400 MHz, CDCl_3) δ 8.71 (s, 1H, -CO-NH-), 8.05 (d, J = 8.0 Hz, 1H, ArH), 7.72 (d, J = 8.8 Hz, 1H, ArH), 7.62 (s, 2H, ArH), 7.29–7.19 (m, 4H, ArH), 7.08 (t, J = 7.4 Hz, 1H, ArH), 6.95 (d, J = 8.4 Hz, 1H, Ph-CO-CH=CH-), 6.70 (d, J = 10.0 Hz, 1H, Ph-CO-CH=CH-), 6.51 (d, J = 8.9 Hz, 1H, Ph-CH=CH-C(CH₃)₂), 5.63 (d, J = 10.0 Hz, 1H, Ph-CH=CH-C(CH₃)₂), 4.67 (s, 2H, -O-CH₂-CO-NH-), 3.92 (s, 3H, -OCH₃), 3.88 (s, 3H, -OCH₃), 2.32 (s, 3H, -CH₃), 1.51 (s, 6H, 2 × -CH₃). ^{13}C NMR (100 MHz, CDCl_3) δ 189.65, 165.94, 158.46, 153.66, 151.22, 147.07, 140.50, 135.18, 131.70, 130.50, 129.07, 128.61, 128.17, 126.91, 126.15, 125.08, 124.52, 121.91, 121.66, 116.83, 113.29, 111.89, 110.50, 103.55, 69.08, 55.91, 55.81, 28.10, 17.34. HR-MS (m/z) (ESI): calcd for $\text{C}_{31}\text{H}_{31}\text{O}_6\text{N}$ [$\text{M}+\text{H}^+$]: 514.22296; found: 514.21447.

Compound 7j: yield, 54.5%; ^1H NMR (400 MHz, CDCl_3) δ 9.28 (s, 1H, -CO-NH-), 8.43 (d, J = 8.3 Hz, 1H, ArH), 7.72 (d, J = 8.8 Hz, 1H, ArH), 7.61 (d, J = 0.8 Hz, 2H, ArH), 7.58–7.56 (m, 1H, ArH), 7.39–7.20 (m, 4H, ArH), 7.04–7.00 (m, 1H, ArH), 6.96 (d, J = 8.4 Hz, 1H, Ph-CO-CH=CH-), 6.70 (d, J = 10.0 Hz, 1H, Ph-CO-CH=CH-), 6.52 (d, J = 8.9 Hz, 1H, Ph-CH=CH-C(CH₃)₂), 5.63 (d, J = 10.0 Hz, 1H, Ph-CH=CH-C(CH₃)₂), 4.68 (s, 2H, -O-CH₂-CO-NH-), 3.93 (s, 3H, -OCH₃), 3.88 (s, 3H, -OCH₃), 1.50 (s, 6H, 2 × -CH₃). ^{13}C NMR (100 MHz, CDCl_3) δ 189.71, 166.36, 158.44, 153.64, 151.50, 147.01, 140.59, 135.19, 132.49, 131.70, 128.93, 128.61, 128.40, 126.09, 125.60, 124.70, 121.89,

121.70, 116.82, 113.71, 113.67, 111.99, 110.48, 103.53, 69.18, 55.93, 55.81, 28.09. HR-MS (m/z) (ESI): calcd for $C_{30}H_{28}O_6NBr$ [$M+Na^+$]:602.09772; found: 602.08456.

Compound **7k**: yield, 52.3%; 1H NMR (400 MHz, $CDCl_3$) δ 9.34 (s, 1H, -CO-NH-), 8.46 (d, $J = 7.7$ Hz, 1H, ArH), 7.72 (d, $J = 8.8$ Hz, 1H, ArH), 7.59 (d, $J = 16.2$ Hz, 2H, ArH), 7.40 (d, $J = 7.7$ Hz, 1H, ArH), 7.32–7.26 (m, 2H, ArH), 7.22 (s, 1H, ArH), 7.16–6.92 (m, 3H, ArH, Ph-CO-CH=CH-, overlapped signals), 6.70 (d, $J = 10.0$ Hz, 1H, Ph-CO-CH=CH-), 6.52 (d, $J = 8.8$ Hz, 1H, Ph-CH=CH-C(CH₃)₂), 5.63 (d, $J = 10.0$ Hz, 1H, Ph-CH=CH-C(CH₃)₂), 4.68 (s, 2H, -O-CH₂-CO-NH-), 3.91 (d, $J = 19.9$ Hz, 6H, 2 \times -OCH₃), 1.50 (s, 6H, 2 \times -CH₃). ^{13}C NMR (100 MHz, $CDCl_3$) δ 189.69, 166.34, 158.43, 153.63, 151.50, 147.05, 140.56, 134.08, 131.69, 129.21, 128.94, 128.60, 127.75, 126.09, 125.05, 124.70, 123.25, 121.69, 121.54, 116.81, 113.77, 111.97, 110.48, 103.52, 69.26, 55.92, 55.80, 28.08. HR-MS (m/z) (ESI): calcd for $C_{30}H_{28}O_6NCl$ [$M+H^+$]:534.16834; found:534.15718.

Compound **7l**: yield, 65.3%; 1H NMR (400 MHz, $CDCl_3$) δ 9.15 (s, 1H, -CO-NH-), 8.42–8.37 (m, 1H, ArH), 7.72 (d, $J = 8.8$ Hz, 1H, ArH), 7.61 (s, 2H, ArH), 7.31–7.24 (m, 2H, ArH), 7.17–7.07 (m, 3H, ArH), 6.96 (d, $J = 8.4$ Hz, 1H, Ph-CO-CH=CH-), 6.70 (d, $J = 10.0$ Hz, 1H, Ph-CO-CH=CH-), 6.52 (d, $J = 8.9$ Hz, 1H, Ph-CH=CH-C(CH₃)₂), 5.63 (d, $J = 10.0$ Hz, 1H, Ph-CH=CH-C(CH₃)₂), 4.69 (s, 2H, -O-CH₂-CO-NH-), 3.96 (s, 3H, -OCH₃), 3.88 (s, 3H, -OCH₃), 1.51 (s, 6H, 2 \times -CH₃). ^{13}C NMR (100 MHz, $CDCl_3$) δ 189.66, 166.60, 158.45, 153.65, 151.64, 147.42, 140.47, 131.71, 129.07, 128.60, 126.16, 125.86, 125.76, 124.91, 124.82, 124.75, 124.63, 121.68, 121.67, 116.82, 115.05, 114.86, 114.80, 112.01, 110.48, 103.54, 70.13, 56.00, 55.81, 28.09. HR-MS (m/z) (ESI): calcd for $C_{30}H_{28}O_6NF$ [$M+H^+$]:518.19789; found:518.18747.

Compound **12a**: yield, 93.5%; 1H NMR (400 MHz, $CDCl_3$) δ 8.83 (s, 1H, -CO-NH-), 7.75 (d, $J = 15.5$ Hz, 1H, ArH), 7.61 (d, $J = 8.0$ Hz, 2H, ArH), 7.38–7.33 (m, 4H, ArH), 7.29 (d, $J = 1.5$ Hz, 1H, Ph-CO-CH=CH-), 7.27 (s, 2H, ArH), 7.15 (t, $J = 7.4$ Hz, 1H, ArH), 6.98 (d, $J = 8.4$ Hz, 1H, Ph-CO-CH=CH-), 4.70 (s, 2H, -O-CH₂-CO-NH-), 3.98 (s, 3H, -OCH₃), 3.94 (d, $J = 2.1$ Hz, 9H, 3 \times -OCH₃). ^{13}C NMR (100 MHz, $CDCl_3$) δ 188.95, 166.43, 153.18, 152.02, 147.47, 143.85, 142.55, 137.13, 133.57, 129.12, 128.45, 125.52, 124.76, 120.33, 119.90, 115.23, 112.09, 106.14, 70.31, 60.99, 56.47, 56.15. HR-MS (m/z) (ESI): calcd for $C_{27}H_{27}O_7N$ [$M+Na^+$]:500.16852; found:500.15859.

Compound **12b**: yield, 95.6%; 1H NMR (400 MHz, $CDCl_3$) δ 8.70 (s, 1H, -CO-NH-), 7.75 (d, $J = 15.6$ Hz, 1H, ArH), 7.52–7.50 (m, 2H, ArH), 7.37–7.33 (m, 2H, ArH), 7.29 (d, $J = 1.9$ Hz, 1H, Ph-CO-CH=CH-), 7.27 (s, 2H, ArH), 6.98 (d, $J = 8.4$ Hz, 1H, Ph-CO-CH=CH-), 6.90–6.88 (m, 2H, ArH), 4.70 (s, 2H, -O-CH₂-CO-NH-), 3.98 (s, 3H, -OCH₃), 3.95 (d, $J = 3.2$ Hz, 9H, 3 \times -OCH₃), 3.80 (s, 3H, -OCH₃). ^{13}C NMR (100 MHz, $CDCl_3$) δ 188.95, 166.16, 156.74, 153.18, 152.00, 147.48, 143.89, 142.55, 133.58, 130.21, 128.43, 125.47, 121.69, 120.30, 115.04, 114.27, 112.06, 106.13, 70.20, 60.99, 56.47, 56.13, 55.50. HR-MS (m/z) (ESI): calcd for $C_{28}H_{29}O_8N$ [$M+Na^+$]:530.17909; found:530.16858.

Compound **12c**: yield, 94.5%; 1H NMR (400 MHz, $CDCl_3$) δ 8.74 (s, 1H, -CO-NH-), 7.75 (d, $J = 15.6$ Hz, 1H, ArH), 7.49–7.47 (m, 2H, ArH), 7.37–7.33 (m, 2H, ArH), 7.29 (d, $J = 1.9$ Hz, 1H, Ph-CO-CH=CH-), 7.27 (s, 2H, ArH), 7.16 (d, $J = 8.2$ Hz, 2H, ArH), 6.98 (d, $J = 8.4$ Hz, 1H, Ph-CO-CH=CH-), 4.70 (s, 2H, -O-CH₂-CO-NH-), 3.98 (s, 3H, -OCH₃), 3.94 (d, $J = 3.1$ Hz, 9H, 3 \times -OCH₃), 2.33 (s, 3H, -CH₃). ^{13}C NMR (100 MHz, $CDCl_3$) δ 188.97, 166.27, 153.18, 152.02, 147.49, 143.89 (s), 142.55, 134.55, 134.45, 133.58, 129.61, 128.44, 125.52, 120.31, 119.97, 115.10, 112.06, 106.13, 70.28, 60.99, 56.47, 56.13, 20.91. HR-MS (m/z) (ESI): calcd for $C_{28}H_{29}O_7N$ [$M+Na^+$]:514.18417; found:514.17419.

Compound **12d**: yield, 91.2%; 1H NMR (400 MHz, $CDCl_3$) δ 8.80 (s, 1H, -CO-NH-), 7.67 (d, $J = 15.6$ Hz, 1H, ArH), 7.45 (d, $J = 8.9$ Hz, 2H, ArH), 7.39 (d, $J = 8.9$ Hz, 2H, ArH), 7.31–7.24 (m, 2H, ArH), 7.21 (d, $J = 1.4$ Hz, 1H, Ph-CO-CH=CH-), 7.19 (s, 2H, ArH), 6.92 (d, $J = 8.4$ Hz, 1H, Ph-CO-CH=CH-), 4.62 (s, 2H, -O-CH₂-CO-NH-), 3.91 (s, 3H, -OCH₃), 3.87 (d, $J = 4.0$ Hz, 9H, 3 \times -OCH₃). ^{13}C NMR (100 MHz,

$CDCl_3$) δ 189.00, 166.53, 153.19, 151.95, 147.37, 143.81, 142.61, 136.23, 133.54, 132.11, 128.53, 125.55, 121.42, 120.43, 117.38, 115.45, 112.17, 106.18, 70.32, 61.00, 56.49, 56.18. HR-MS (m/z) (ESI): calcd for $C_{27}H_{26}O_7NBr$ [$M+Na^+$]: 580.07669; found:580.06663.

Compound **12e**: yield, 90.5%; 1H NMR (400 MHz, $CDCl_3$) δ 8.88 (s, 1H, -CO-NH-), 7.77–7.33 (m, 1H, ArH), 7.64–7.52 (m, 2H, ArH), 7.41–7.24 (m, 7H, ArH, Ph-CO-CH=CH-, Ph-CO-CH=CH-, overlapped signals), 7.00–6.97 (m, 1H, ArH), 4.70 (s, 2H, -O-CH₂-CO-NH-), 3.99–3.95 (m, 12H, 4 \times -OCH₃). ^{13}C NMR (100 MHz, $CDCl_3$) δ 188.92, 166.47, 153.18, 151.97, 147.38, 143.75, 142.62, 135.75, 133.53, 129.72, 129.13, 128.51, 125.50, 121.07, 120.41, 115.50, 112.15, 106.19, 70.31, 60.97, 56.46, 56.15. HR-MS (m/z) (ESI): calcd for $C_{27}H_{26}O_7NCl$ [$M+Na^+$]:534.12955; found:534.11949.

Compound **12f**: yield, 89.0%; 1H NMR (400 MHz, $CDCl_3$) δ 8.81 (s, 1H, -CO-NH-), 7.73 (d, $J = 15.5$ Hz, 1H, ArH), 7.58–7.54 (m, 2H, ArH), 7.36–7.32 (m, 2H, ArH, Ph-CO-CH=CH-, overlapped signals), 7.27 (s, 1H, ArH), 7.25 (s, 2H, ArH), 7.03 (t, $J = 8.6$ Hz, 2H, ArH), 6.97 (d, $J = 8.4$ Hz, 1H, Ph-CO-CH=CH-), 4.68 (s, 2H, -O-CH₂-CO-NH-), 3.96 (s, 3H, -OCH₃), 3.93 (d, $J = 2.1$ Hz, 9H, 3 \times -OCH₃). ^{13}C NMR (100 MHz, $CDCl_3$) δ 188.94, 166.40, 160.81, 158.39, 153.18, 151.97, 147.39, 143.82, 142.58, 133.54, 133.19, 133.17, 128.48, 125.48, 121.71, 121.63, 120.37, 115.89, 115.67, 115.35, 112.13, 106.16, 70.22, 60.98, 56.47, 56.16. HR-MS (m/z) (ESI): calcd for $C_{27}H_{26}O_7NF$ [$M+Na^+$]:518.15910; found:518.14944.

Compound **12g**: yield, 87.6%; 1H NMR (400 MHz, $DMSO-d_6$) δ 9.78 (s, 1H, -CO-NH-), 9.26 (s, 1H, -OH), 7.84–7.66 (m, 2H, ArH), 7.60–7.49 (m, 2H, ArH), 7.44–7.34 (m, 4H, ArH), 7.10 (d, $J = 8.4$ Hz, 1H, Ph-CO-CH=CH-), 6.71 (d, $J = 8.7$ Hz, 2H, ArH, Ph-CO-CH=CH-, overlapped signals), 4.74 (s, 2H, -O-CH₂-CO-NH-), 3.88 (s, 9H, 3 \times -OCH₃), 3.76 (s, 3H, -OCH₃). ^{13}C NMR (100 MHz, $DMSO-d_6$) δ 188.35, 166.25, 154.22, 153.36, 152.07, 148.03, 144.46, 142.39, 133.73, 130.33, 128.00, 124.98, 121.85, 120.36, 115.61, 114.65, 112.75, 106.65, 69.15, 60.67, 56.69, 56.30. HR-MS (m/z) (ESI): calcd for $C_{27}H_{27}O_8N$ [$M+Na^+$]:516.16344; found:516.15421.

Compound **12h**: yield, 82.3%; 1H NMR (400 MHz, $CDCl_3$) δ 9.14 (s, 1H, -CO-NH-), 8.32 (d, $J = 8.0$ Hz, 1H, ArH), 7.68 (d, $J = 15.6$ Hz, 1H, ArH), 7.29–7.24 (m, 2H, ArH), 7.21 (d, $J = 1.9$ Hz, 1H, Ph-CO-CH=CH-), 7.19 (s, 2H, ArH), 7.04–7.02 (m, 1H, ArH), 6.93–6.89 (m, 2H, ArH), 6.84 (d, $J = 8.1$ Hz, 1H, Ph-CO-CH=CH-), 4.63 (s, 2H, -O-CH₂-CO-NH-), 3.90 (s, 3H, -OCH₃), 3.87 (d, $J = 3.3$ Hz, 9H, 3 \times -OCH₃), 3.83 (s, 3H, -OCH₃). ^{13}C NMR (100 MHz, $CDCl_3$) δ 189.07, 166.17, 153.18, 152.15, 148.45, 147.31, 144.13, 142.51, 133.63, 128.17, 126.84, 125.31, 124.45, 121.13, 120.15, 114.24, 112.05, 110.28, 106.12, 69.61, 60.99, 56.47, 56.09, 55.89. HR-MS (m/z) (ESI): calcd for $C_{28}H_{29}O_8N$ [$M+Na^+$]:530.17909; found:530.16653.

Compound **12i**: yield, 75.5%; 1H NMR (400 MHz, $CDCl_3$) δ 8.68 (s, 1H, -CO-NH-), 8.02 (d, $J = 8.0$ Hz, 1H, ArH), 7.76 (d, $J = 15.5$ Hz, 1H, ArH), 7.38–7.32 (m, 2H, ArH), 7.27 (s, 2H), 7.26–7.20 (m, 3H, ArH, Ph-CO-CH=CH-, overlapped signals), 7.10 (t, $J = 7.5$ Hz, 1H, ArH), 6.97 (d, $J = 8.4$ Hz, 1H, Ph-CO-CH=CH-), 4.73 (s, 2H, -O-CH₂-CO-NH-), 3.95 (d, $J = 3.3$ Hz, 12H, 4 \times -OCH₃), 2.32 (s, 3H, -CH₃). ^{13}C NMR (100 MHz, $CDCl_3$) δ 188.99, 166.09, 153.18, 151.77, 147.11, 144.02, 142.56, 135.05, 133.59, 130.54, 128.37, 128.22, 126.93, 125.24, 125.20, 122.08, 120.1, 113.45, 111.86, 106.15, 69.14, 60.99, 56.47, 55.96, 17.35. HR-MS (m/z) (ESI): calcd for $C_{28}H_{29}O_7N$ [$M+Na^+$]:514.18417; found:514.17411.

Compound **12j**: yield, 53.5%; 1H NMR (400 MHz, $CDCl_3$) δ 9.26 (s, 1H, -CO-NH-), 8.43 (d, $J = 7.5$ Hz, 1H, ArH), 7.76 (d, $J = 15.5$ Hz, 1H, ArH), 7.62–7.53 (m, 1H, ArH), 7.39–7.32 (m, 3H, ArH, Ph-CO-CH=CH-, overlapped signals), 7.28 (s, 1H, ArH), 7.27 (s, 2H, ArH), 7.04–7.01 (m, 1H, ArH), 6.98 (d, $J = 8.3$ Hz, 1H, Ph-CO-CH=CH-), 4.73 (s, 2H, -O-CH₂-CO-NH-), 3.95–3.94 (m, 12H, 4 \times -OCH₃). ^{13}C NMR (100 MHz, $CDCl_3$) δ 188.98, 166.43, 153.18, 152.11, 147.08, 144.06, 142.53, 135.12, 133.63, 132.50, 128.45, 128.08, 125.68, 125.43, 121.91, 120.13, 114.10, 113.67, 111.99, 106.13, 69.37, 60.99,

56.48, 55.98. HR-MS (m/z) (ESI): calcd for $C_{27}H_{26}O_7NBr$ [$M+Na^+$]:580.07669; found:580.06677.

Compound **12k**: yield, 43.1%; 1H NMR (400 MHz, $CDCl_3$) δ 9.31 (s, 1H, -CO-NH-), 8.46 (d, $J = 8.3$ Hz, 1H, ArH), 7.76 (d, $J = 15.6$ Hz, 1H, ArH), 7.42–7.39 (m, 1H, ArH), 7.37–7.31 (m, 3H, ArH), 7.29–7.27 (m, 4H, ArH, Ph-CO-CH=CH-, overlapped signals), 7.09 (t, $J = 7.7$ Hz, 1H), 6.97 (d, $J = 8.4$ Hz, 1H, Ph-CO-CH=CH-), 4.73 (s, 2H, -O-CH₂-CO-NH-), 3.95 (s, 6H, 2 \times -OCH₃, overlapped signals), 3.95 (d, $J = 1.9$ Hz, 6H, 2 \times -OCH₃). ^{13}C NMR (100 MHz, $CDCl_3$) δ 188.98, 166.40, 153.18, 152.11, 147.10, 144.05, 142.53, 134.02, 133.62, 129.22, 128.09, 127.80, 125.42, 125.14, 123.24, 121.57, 120.12, 114.12, 111.96, 106.13, 69.42, 60.99, 56.47, 55.97. HR-MS (m/z) (ESI): calcd for $C_{27}H_{26}O_7NCl$ [$M+Na^+$]:534.12955; found:534.11866.

Compound **12l**: yield, 63.3%; 1H NMR (400 MHz, $CDCl_3$) δ 9.11 (s, 1H, -CO-NH-), 7.41–7.36 (m, 1H, ArH), 7.75 (d, $J = 15.5$ Hz, 1H, ArH), 7.38–7.33 (m, 2H, ArH), 7.30 (d, $J = 1.7$ Hz, 1H, Ph-CO-CH=CH-), 7.28 (s, 2H, ArH), 7.17–7.08 (m, 3H, ArH), 6.97 (d, $J = 8.4$ Hz, 1H, Ph-CO-CH=CH-), 4.73 (s, 2H, -O-CH₂-CO-NH-), 3.97 (s, 3H, -OCH₃), 3.95 (d, $J = 4.1$ Hz, 9H, 3 \times -OCH₃). ^{13}C NMR (100 MHz, $CDCl_3$) δ 188.96, 166.63, 153.84, 153.18, 152.22, 151.41, 147.43, 143.94, 142.54, 133.61, 128.22, 125.77, 125.67, 125.58, 124.92, 124.84, 124.66, 124.62, 121.73, 120.21, 115.07, 114.88, 111.99, 106.14, 70.21, 60.98, 56.46, 56.03. HR-MS (m/z) (ESI): calcd for $C_{27}H_{26}O_7NF$ [$M+Na^+$]:518.15910; found:518.14879.

4.2. Cell culture and maintenance

All human cancer cell lines and human normal liver cell line HL-7702 in this study were purchased from China Life Science Collage (Shanghai, PRC). Culture medium Dulbecco's modified Eagle medium (DMEM), fetal bovine serum (FBS), phosphate buffered saline (PBS, pH = 7.2), and Antibiotic-Antimycotic came from KeyGen Biotech Company (China). Cell lines were grown in the supplemented with 10% FBS, 100 units/ml of penicillin and 100 g/mL of streptomycin in a humidified atmosphere of 5% CO₂ at 37 °C.

4.3. Cytotoxicity assay

The anticancer activity of the all compounds were investigated in five human cancer cell lines (HepG-2, NCI-H460, MGC-803, SK-OV-3 and T24) and human normal liver cell line (HL-7702). Among all compounds, compound **12k** was further evaluated on paclitaxel resistance cancer cell lines (A549 and HeLa). About 1×10^5 cells/mL cells, which were in the logarithmic phase, were grown in each well of 96-well plates and incubated for 12 h of 5% CO₂ at 37 °C. All compounds at five different concentrations were then added to the test well and the cells were incubated at 37 °C in a 5% CO₂ atmosphere for 48 h, respectively. An enzyme labeling instrument was used to read absorbance with 570/630 nm double wavelength measurement. Cytotoxicity was evaluated on the percentage of cell survival compared with control group. The final IC₅₀ values were calculated by the Bliss method ($n = 5$). All of the tests were repeated in triplicate.

4.4. Tubulin polymerization assay in vitro assays

Tubulin polymerization assay was monitored by the change in optical density at 340 nm using a modification of methods described by Jordan et al. [50] Purified brain tubulin polymerization kit was purchased from Cytoskeleton (BK006P, Denver, CO). The final buffer concentrations for tubulin polymerization contained 80.0 mM piperazine-*N,N'*-bis(2-ethanesulfonic acid)sequisodium salt (pH = 6.9), 2.0 mM MgCl₂, 0.5 mM ethylene glycol bis(β -aminoethyl

ether)-*N,N,N',N'*-tetraacetic acid (EGTA), 1 mM GTP, and 10.2% glycerol. Test compounds were added in different concentrations, and then all components except the purified tubulin were warmed to 37 °C. The reaction was initiated by the addition of tubulin to a final concentration of 3.0 mg/mL. Paclitaxel was used as positive controls under the same conditions. The optical density was measured for 40 min at 1 min intervals in BioTek's Synergy 4 multifunction microplate spectrophotometer with a temperature controlled cuvette holder. Assays were performed according to the manufacturer's instructions and under conditions similar to those employed for the tubulin polymerization assays described above [8,51].

4.5. Molecular docking

All the docking studies were carried out using Sybyl-X 2.0 on a windows workstation. The crystal structure of the tubulin in complex with colchicine was retrieved from the RCSB Protein Data Bank (PDB: 1SA0.pdb) [52]. The synthetic chalcone analogues were selected for the docking studies. The 3D structures of these selected compounds were first built using Sybyl-X 2.0 sketch followed by energy minimization using the MMFF94 force field and Gasteiger-Marsili charges. We employed Powell's method for optimizing the geometry with a distance dependent dielectric constant and a termination energy gradient of 0.005 kcal/mol. All the selected compounds were automatically docked into the colchicine binding pocket of tubulin by an empirical scoring function and a patented search engine in the Surflex docking program. The polar hydrogen atoms were added and also the automated docking manner was applied in the present work. Other parameters were established by default to estimate the binding affinity characterized by the Surflex-Dock scores in the software. Surflex-Dock total scores, which were expressed in -log₁₀ (Kd) units to represent binding affinities, were applied to evaluate the ligand-receptor interactions of newly designed molecules. A higher score represents stronger binding affinity. The optimal binding pose of the docked compounds was selected based on the Surflex scores and visual inspection of the docked complexes.

4.6. Flow cytometry analysis of cell cycle distribution

The NCI-H460 cells were grown on 6-well plates and treated with compound **12k** (5, 10 μ M), and maintained with the proper culture medium in 5% CO₂ at 37 °C for 24 h. After completion of incubation, cells were harvested and washed twice with ice-cold PBS, fixed with ice-cold 70% ethanol at -20 °C for overnight. The cells were treated with 100 μ g/mL RNase A for 30 min at 37 °C after washed with twice ice-cold PBS, and finally stained with 1 mg/mL propidium iodide (PI) in the dark at 4 °C for 1 h. Analysis was performed with the system software (Cell Quest; BD Biosciences).

4.7. Apoptosis analysis

Apoptosis was examined by flow cytometry analysis of annexin V/PI staining. NCI-H460 cells were seeded in each well of 96-well plates at the density of 1×10^5 cells/mL of the DMEM medium with 10% FBS to the final volume of 2 mL. The plates were incubated for overnight and treated with different concentrations of the test compound **12k** for 24 h. Briefly, cells were harvested and washed with three times ice-cold PBS, and then suspended cells in the annexin-binding buffer at a concentration of 5×10^5 cells/ml. cells were then incubated with 5 μ L of annexin V-FITC and 5 μ L of PI for 30 min at room temperature in the dark. The cells were analyzed by system software (Cell Quest; BD Biosciences).

4.8. Mitochondrial membrane potential assay

The mitochondrial membrane potential was measured by flow cytometry using the JC-1 fluorescent probe (Beyotime, Haimen, China, Molecular Probe), as previously described [53]. NCI-H460 cells were treated with different concentrations of the test compound **12k** for 24 h. After for 24 h, the JC-1 fluorescent probe was added 20 min after replacing with fresh medium. Cells were harvested at 2000 rpm and washed twice with ice-cold PBS and the loss of mitochondrial membrane potential were investigated by flow cytometry. The emission fluorescence for JC-1 was monitored at 530 and 590 nm, under the excitation wavelength at 488 nm, respectively.

4.9. ROS assay

The production of ROS was examined by flow cytometry using DCFH-DA (Molecular Probe, Beyotime, Haimen, China), as previously described [53]. NCI-H460 cells were grown into six-well plates and subjected to various treatments. On the following treatment, cells were collected at 2000 rpm and washed twice with ice-cold PBS, and then resuspend cells in 10 mM DCFH-DA dissolved in cell free medium at 37 °C for 20 min in dark, and then washed twice with ice-cold PBS. Cellular fluorescence was analyzed by flow cytometry at an excitation of 485 nm and an emission of 538 nm.

4.10. Western blot analysis

Western blot analysis was performed as described previously [52]. NCI-H460 cells were treated with different concentrations of the test compound **12k** for 48 h. After that time, cells were harvested, centrifuged, and washed twice with ice-cold PBS. The pellet was then resuspended in lysis buffer. After the cells were lysed on ice for 20 min, lysates were centrifuged at 20000 g at 4 °C for 5 min. The protein concentration in the supernatant was analyzed using the BCA protein assay reagents (Imgenex, USA). Equal amounts of protein per line were separated on 12% SDS polyacrylamide gel electrophoresis and transferred to PVDF Hybond-P membrane (GE Healthcare). Membranes were incubated with 5% skim milk in Tris-buffered saline with Tween 20 (TBST) buffer for 1 h and then the membranes being gently rotated overnight at 4 °C. Membranes were then incubated with primary antibodies against Bcl-2, Bax, Cyt c, caspase-9, caspase-3, or β -actin for overnight at 4 °C. Membranes were next incubated with peroxidase labeled secondary antibodies for 2 h. Then all membranes were washed with TBST three times for 15 min and the protein blots were investigated with chemiluminescence reagent (Thermo Fischer Scientifics Ltd.). The X-ray films were developed with developer and fixed with fixer solution.

4.11. Statistical analysis

All statistical analysis was performed with SPSS Version 10. Data was analyzed by one-way ANOVA. Mean separations were performed using the least significant difference method. Each experiment was replicated thrice, and all experiments yielded similar results. Measurements from all the replicates were combined, and treatment effects were analyzed.

Acknowledgments

We are grateful to the National Natural Science Foundation of China (Grant No. 21571033) for financial aid to this work. The authors would also like to thank the Fundamental Research Funds for

the Central Universities (Project 2242016K30020) for supplying basic facilities to our key laboratory. We also want to express our gratitude to the Priority Academic Program Development of Jiangsu Higher Education Institutions for the construction of fundamental facilities (Project 1107047002). Huang is grateful to the Innovation Program of Jiangsu Province postgraduate education (Project KYLX16_0263). The research was also supported by the Scientific Research Foundation of Graduated School of Southeast University (YBJJ1677).

Appendix A. Supplementary data

Supplementary data related to this article can be found at <http://dx.doi.org/10.1016/j.ejmech.2017.03.031>.

References

- [1] J. Seligmann, C. Twelves, Tubulin: an example of targeted chemotherapy, *Future Med. Chem.* 5 (2013) 339–352.
- [2] R.A. Stanton, K.M. Gernert, J.H. Nettles, R. Aneja, Drugs that target dynamic microtubules: a new molecular perspective, *Med. Res. Rev.* 31 (2011) 443–481.
- [3] Y.V. Voitovich, E.S. Shegravina, N.S. Sitnikov, V.I. Faerman, V.V. Fokin, H.G. Schmalz, S. Combes, D. Allegro, P. Barbier, I.P. Beletskaya, E.V. Svirshchevskaya, A.Y. Fedorov, Synthesis and biological evaluation of furanocolchiclinoids, *J. Med. Chem.* 58 (2015) 692–704.
- [4] M. Kavallaris, Microtubules and resistance to tubulin-binding agents, *Nat. Rev. Cancer* 10 (2010) 194–204.
- [5] R. Romagnoli, P.G. Baraldi, M.K. Salvador, D. Preti, M.A. Tabrizi, A. Brancale, X.H. Fu, J. Li, S.Z. Zhang, E. Hamel, R. Bortolozzi, E. Porcú, G. Basso, G. Viola, Discovery and optimization of a series of 2-Aryl-4-Amino-5-(3',4',5'-trime-thoxybenzoyl) thiazoles as novel anticancer agents, *J. Med. Chem.* 55 (2012) 5433–5445.
- [6] J.R. McIntosh, E. Grishchuk, R.R. West, Chromosome-microtubule interactions during mitosis, *Annu. Rev. Cell Dev. Biol.* 18 (2002) 193–219.
- [7] R. Heald, E. Nogales, Microtubule dynamics, *J. Cell Sci.* 115 (2002) 3–4.
- [8] P.B. Schiff, J. Fant, S.B. Horwitz, Promotion of microtubule assembly *in vitro* by taxol, *Nature* 277 (1979) 665–667.
- [9] R. Kaur, G. Kaur, R.K. Gill, R. Soni, J. Bariwal, Recent developments in tubulin polymerization inhibitors: an overview, *Eur. J. Med. Chem.* 87 (2014) 89–124.
- [10] Q.X. Yue, X. Liu, D.A. Guo, Microtubule-binding natural products for cancer therapy, *Planta Med.* 76 (2010) 1037–1043.
- [11] M.A. Jordan, L. Wilson, Microtubules as a target for anticancer drugs, *Nat. Rev. Cancer* 4 (2004) 253–265.
- [12] B. Gigant, C. Wang, R.B. Ravelli, F. Roussi, M.O. Steinmetz, P.A. Curmi, A. Sobel, M. Knossow, Structural basis for the regulation of tubulin by vinblastine, *Nature* 435 (2005) 519–522.
- [13] J. Löwe, H. Li, K.H. Downing, E. Nogales, Refined structure of $\alpha\beta$ -tubulin at 3.5 Å resolution, *J. Mol. Biol.* 313 (2001) 1045–1057.
- [14] M.A. Jordan, L. Wilson, Microtubules as a target for anticancer drugs, *Nat. Rev. Cancer* 4 (2004) 253–265.
- [15] G.C. Wang, C.Y. Li, L. He, K. Lei, F. Wang, Y.Z. Pu, Z. Yang, D. Cao, L. Ma, J.Y. Chen, Y. Sang, X.L. Liang, M.L. Xiang, A.H. Peng, Y.Q. Wei, L.J. Chen, Design, synthesis and biological evaluation of a series of pyrano chalcone derivatives containing indole moiety as novel anti-tubulin agents, *Bioorg. Med. Chem.* 22 (2014) 2060–2079.
- [16] M. Alami, S. Messaoudi, B. Treguiet, A. Hamze, O. Provot, J.F. Peyrat, J.R. De Losada, J.M. Liu, J. Bignon, J. Wdzieczak-Bakala, S. Thoret, J. Dubois, J.D. Brion, Iso combretastatins A versus combretastatins A: the forgotten iso CA-4 isomer as a highly promising cytotoxic and antitubulin agent, *J. Med. Chem.* 52 (2009) 4538–4542.
- [17] D.J. Newman, G.M. Cragg, K.M. Snader, Natural products as sources of new drugs over the period 1981–2002, *J. Nat. Prod.* 66 (2003) 1022–1037.
- [18] B. Zhang, D. Duan, C. Ge, J. Yao, Y. Liu, X. Li, J. Fang, Synthesis of xanthohumol analogues and discovery of potent thioredoxin reductase inhibitor as potential anticancer agent, *J. Med. Chem.* 58 (2015) 1795–1805.
- [19] W. Cai, B. Zhang, D. Duan, J. Wu, J. Fang, Curcumin targeting the thioredoxin system elevates oxidative stress in HeLa cells, *Toxicol. Appl. Pharmacol.* 262 (2012) 341–348.
- [20] N.K. Sahu, S.S. Ballhadra, J. Choudhary, D.V. Kohli, Exploring pharmacological significance of chalcone scaffold: a review, *Curr. Med. Chem.* 19 (2012) 209–225.
- [21] Z. Yang, W. Wu, J. Wang, L. Liu, L. Li, J. Yang, G. Wang, D. Cao, R. Zhang, M. Tang, J. Wen, J. Zhu, W. Xiang, F. Wang, L. Ma, M. Xiang, J. You, L.J. Chen, Synthesis and biological evaluation of novel millepachine derivatives as a new class of tubulin polymerization inhibitors, *J. Med. Chem.* 57 (2014) 7977–7989.
- [22] J. Chen, J. Yan, J. Hu, Y. Pang, L. Huang, X. Li, Synthesis, biological evaluation and mechanism study of chalcone analogues as novel anti-cancer agents, *RSC Adv.* 5 (2015) 68128–68135.

- [23] D. Kumar, N.M. Kumar, K. Akamatsu, E. Kusaka, H. Harada, T. Ito, Synthesis and biological evaluation of indolyl chalcones as antitumor agents, *Bioorg. Med. Chem. Lett.* 20 (2010) 3916–3919.
- [24] M.L. Edwards, D.M. Stemerick, P.S. Sunkara, Chalcones: a new class of anti-mitotic agents, *J. Med. Chem.* 133 (1990) 1948–1954.
- [25] S. Ducki, D. Rennison, M. Woo, A. Kendall, J.F.D. Chabert, A.T. McGown, N.J. Lawrence, Combretastatin-like chalcones as inhibitors of microtubule polymerization. Part 1: synthesis and biological evaluation of anti-vascular activity, *Bioorg. Med. Chem.* 17 (2009) 7698–7710.
- [26] S.P. Bahekar, S.V. Hande, N.R. Agrawal, H.S. Chandak, P.S. Bhoj, K. Goswami, M.V.R. Reddy, Sulfonamide chalcones: synthesis and *in vitro* exploration for therapeutic potential against *Brugia malayi*, *Eur. J. Med. Chem.* 124 (2016) 262–269.
- [27] K.H. Jeon, Lee, E.K.Y. Jun, J.E. Eom, S.Y. Kwak, Y. Na, Y. Kwon, Neuroprotective effect of synthetic chalcone derivatives as competitive dual inhibitors against m-calpain and cathepsin B through the downregulation of tau phosphorylation and insoluble Ab peptide formation, *Eur. J. Med. Chem.* 121 (2016) 433–444.
- [28] T. Kraege, K. Stefan, K. Juvalle, T. Ross, T. Willmes, M. Wiese, The combination of quinazoline and chalcone moieties leads to novel potent heterodimeric modulators of breast cancer resistance protein (BCRP/ABCG2), *Eur. J. Med. Chem.* 117 (2016) 212–229.
- [29] A. Hammuda, R. Shalaby, S. Rovida, Edmondson, D.E.C. Binda, A. Khalil, Design and synthesis of novel chalcones as potent selective monoamine oxidase-B inhibitors, *Eur. J. Med. Chem.* 114 (2016) 162–169.
- [30] W. Wu, H. Ye, L. Wan, X. Han, G. Wang, J. Hu, M. Tang, X. Duan, Y. Fan, S. He, L. Huang, H. Pei, X. Wang, X. Li, C. Xie, R. Zhang, Z. Yuan, Y. Mao, Y. Wei, L.J. Chen, Millepachine, a novel chalcone, induces G2/M arrest by inhibiting CDK1 activity and causing apoptosis via ROS-mitochondrial apoptotic pathway in human hepatocarcinoma cells *in vitro* and *in vivo*, *Carcinogenesis* 34 (2013) 1636–1643.
- [31] G. Wang, W. Wu, F. Peng, D. Cao, Z. Yang, L. Ma, N. Qiu, H. Ye, X. Han, J. Chen, J. Qiu, Y. Sang, X. Liang, Y. Ran, A. Peng, Y. Wei, L.J. Chen, Design, synthesis, and structure-activity relationship studies of novel millepachine derivatives as potent antiproliferative agents, *Eur. J. Med. Chem.* 54 (2012) 793–803.
- [32] G. Wang, F. Peng, D. Cao, Z. Yang, X. Han, J. Liu, W. Wu, L. He, L. Ma, J. Chen, Y. Sang, M. Xiang, A. Peng, Y. Wei, L.J. Chen, Design, synthesis and biological evaluation of millepachine derivatives as a new class of tubulin polymerization inhibitors, *Bioorg. Med. Chem.* 21 (2013) 6844–6854.
- [33] B.J. An, S. Zhang, J. Yan, L. Huang, X.S. Li, Synthesis, *in vitro* and *in vivo* evaluation of new hybrids of millepachine and phenstatin as potent tubulin polymerization inhibitors, *Org. Biomol. Chem.* 15 (2017) 852–862.
- [34] S. Ducki, R. Forrest, J.A. Hadfield, A. Kendall, N.J. Lawrence, A.T. McGown, D. Rennison, Potent antimitotic and cell growth inhibitory properties of substituted chalcones, *Bioorg. Med. Chem. Lett.* 8 (1998) 1051–1056.
- [35] R. Schobert, B. Biersack, A. Dietrich, S. Knauer, M. Zoldakova, A. Fruehauf, T. Mueller, Pt(II) complexes of a combretastatin A-4 analogous chalcone: effects of conjugation on cytotoxicity, tumor specificity, and long-term tumor growth suppression, *J. Med. Chem.* 52 (2009) 241–246.
- [36] V. Chaudhary, J.B. Venghateri, H.P.S. Dhaked, A.S. Bhojari, S.K. Guchhait, D. Panda, Novel Combretastatin-2-aminoimidazole analogues as potent tubulin assembly inhibitors: exploration of unique pharmacophoric impact of bridging skeleton and aryl moiety, *J. Med. Chem.* 59 (2016), 3439–345.
- [37] J. Wang, J. Yi, Cancer cell killing via ROS: to increase or decrease, that is the question, *Cancer Biol. Ther.* 7 (2008) 1875–1884.
- [38] Y.L. Chu, C.T. Ho, J.G. Chung, R. Raghun, Y.C. Lo, L.Y. Sheen, Allicin induces anti-human liver cancer cells through the p53 gene modulating apoptosis and autophagy, *J. Agric. Food Chem.* 61 (2013) 9839–9848.
- [39] S.S. Zhang, S.P. Nie, D.F. Huang, Y.L. Feng, M.Y. Xie, A novel polysaccharide from *Ganoderma atrum* exerts antitumor activity by activating mitochondria-mediated apoptotic pathway and boosting the immune system, *J. Agric. Food Chem.* 62 (2014) 1581–1589.
- [40] J.D. Ly, D.R. Grubb, A. Lawen, The mitochondrial membrane potential ($\Delta\psi_m$) in apoptosis: an update, *Apoptosis* 8 (2003) 115–128.
- [41] D.R. Green, G. Kroemer, The pathophysiology of mitochondrial cell death, *Science* 305 (2004) 626–629.
- [42] X.C. Huang, L. Jin, M. Wang, D. Liang, Z.F. Chen, Y. Zhang, Y.M. Pan, H.S. Wang, Design, synthesis and *in vitro* evaluation of novel dehydroabietic acid derivatives containing a dipeptide moiety as potential anticancer agents, *Eur. J. Med. Chem.* 89 (2015) 370–385.
- [43] A. Thorburn, Death receptor-induced cell killing, *Cell. Signal.* 16 (2004) 139–144.
- [44] E. Er, L. Oliver, P.F. Cartron, P. Juin, S. Manon, F.M. Vallette, Mitochondria as the target of the pro-apoptotic protein Bax, *Biochim. Biophys. Acta-Bioenergetics* 1757 (2006) 1301–1311.
- [45] X.C. Huang, R.Z. Huang, Z.X. Liao, Y.M. Pan, S.H. Gou, H.S. Wang, Synthesis and pharmacological evaluation of dehydroabietic acid thiourea derivatives containing bisphosphonate moiety as an inducer of apoptosis, *Eur. J. Med. Chem.* 108 (2016) 381–391.
- [46] X. Jiang, X. Wang, Cytochrome C-mediated apoptosis, *Annu. Rev. Biochem.* 73 (2004) 87–106.
- [47] J.S. Bose, V. Gangan, R. Prakash, S.K. Jain, S.K. Manna, A dihydrobenzofuran lignan induces cell death by modulating mitochondrial pathway and G2/M cell cycle arrest, *J. Med. Chem.* 52 (2009) 3184–3190.
- [48] S.S. Zhang, S.P. Nie, D.F. Huang, Y.L. Feng, M.Y. Xie, A novel polysaccharide from *Ganoderma atrum* exerts antitumor activity by activating mitochondria-mediated apoptotic pathway and boosting the immune system, *J. Agric. Food Chem.* 62 (2014) 1581–1589.
- [49] T. Kuwana, D.D. Newmeyer, Bcl-2-family proteins and the role of mitochondria in apoptosis, *Curr. Opin. Cell Biol.* 15 (2003) 691–699.
- [50] M.A. Jordan, L. Wilson, Microtubules as a target for anticancer drugs, *Nat. Rev. Cancer* 4 (2004) 253–265.
- [51] A.V. Schofield, C. Gamell, R. Suryadinata, B. Sarcevic, O. Bernard, Tubulin polymerization promoting protein 1 (Tppp1) phosphorylation by rho-associated coiled-coil kinase (rock) and cyclin-dependent kinase 1 (Cdk1) inhibits microtubule dynamics to increase cell proliferation, *J. Biol. Chem.* 288 (2013) 7907–7917.
- [52] Y.J. Qin, Y.J. Li, A.Q. Jiang, M.R. Yang, Q.Z. Zhu, H. Dong, H.L. Zhu, Design, synthesis and biological evaluation of novel pyrazoline containing derivatives as potential tubulin assembling inhibitors, *Eur. J. Med. Chem.* 94 (2015) 447–457.
- [53] J.Y. Zhang, T. Yi, J. Liu, Z. Zhao, H.B. Chen, Quercetin induces apoptosis via the mitochondrial pathway in KB and KBv200 cells, *J. Agric. Food Chem.* 61 (2013) 2188–2195.